nature reviews materials

https://doi.org/10.1038/s41578-026-00936-0

Perspective

Check for updates

Irregular metamaterial networks

Thomas P. Wytock[1,2], Chiara Daraio[3], Heinrich M. Jaeger[4,5], Christopher A. Schuh[6], Lorenzo Valdevit[7], Vincenzo Vitelli[4,5,8] & Adilson E. Motter[1,2,9,10]

Abstract

Metamaterials can achieve exceptional functionality through careful design of their mesoscale structure. Although engineered irregularities can be advantageous, current approaches largely conform to regular structures to preserve tractability. Here we contend that network theory, enriched with geometry and physics, provides a natural framework for modelling and designing metamaterials with controlled irregularities at relevant scales. We examine how this augmented network theory can facilitate the creation of irregular metamaterials with enhanced or novel properties and how metamaterial research, in turn, is opening new directions in the broader area of physical networks. Supported by machine learning and advances in self-assembly, the emerging field of irregular metamaterial networks is poised to transform the design and scalable manufacturing of new materials.

Sections

[1]Department of Physics and Astronomy, Northwestern University, Evanston, IL, USA. [2]Center for Network Dynamics, Northwestern University, Evanston, IL, USA. [3]Division of Engineering and Applied Science, California Institute of Technology, Pasadena, CA, USA. [4]Department of Physics, University of Chicago, Chicago, IL, USA. [5]James Franck Institute, University of Chicago, Chicago, IL, USA. [6]Department of Materials Science and Engineering, Northwestern University, Evanston, IL, USA. [7]Department of Materials Science and Engineering, University of California, Irvine, CA, USA. [8]Leinweber Center for Theoretical Physics, University of Chicago, Chicago, IL, USA. [9]Department of Engineering Sciences and Applied Mathematics, Northwestern University, Evanston, IL, USA. [10]Northwestern Institute on Complex Systems, Northwestern University, Evanston, IL, USA. e-mail: motter@northwestern.edu

Introduction

Metamaterials are architected to gain properties from their mesoscopic structure in addition to their microscopic composition, so that they display behaviours that go beyond those of ordinary materials synthesized at the atomic or molecular scale[1]. For example, metamaterials can exhibit high specific strength[2,3], negative refractive index[4], negative Poisson's ratio[5,6] and sound confinement properties[7,8], with respective applications including lightweight aerospace platforms, optical cloaking, mechanical allostery and acoustic superlensing. Traditionally, the mesoscopic structures of metamaterials consist of regular patterns formed by repeating structures with precisely designed form and orientation. However, a new generation of metamaterials with desired properties is being realized by departing from the stringent requirement of regularity (Fig. 1). The key to unlocking the potential of irregular metamaterials is network science.

The study of network systems, the origin of which is often traced to Euler, gained attention in physics after Maxwell's 1864 study of networks of forces[9]. Through the second half of the twentieth century, physical scientists focused largely on regular lattice networks of crystal-like systems, while mathematicians, motivated by the structure of communication networks, developed random graph theory[10]. Over the past 25 years, it has become clear that real physical, biological and social networks tend to fall in between these two extremes: they are irregular but also highly structured and thus by no means random[11,12]. The study of the structure and dynamics of such network systems — ranging from whole-brain connectomes[13–15] and continental-scale power grids[16] to global social media[17,18] and pandemic-related contact networks[19–21] — has given rise to the cross-disciplinary field of network science, which now interacts synergistically with arising artificial intelligence technologies[22,23]. An emerging direction in network theory is to incorporate the physical properties and constraints of network nodes and edges, including how volume exclusion influences structure[24,25], and to design spatially embedded structures with desired dynamics[26] and material properties[27].

Network concepts have been used, often implicitly, in both the analysis and design of materials. The analysis of networks of forces gave rise to the field of topological mechanics[28], which involves the study of how the structure of elements, such as struts, produces robust mechanical behaviours. In this context, rigidity has been formulated as a vector percolation problem and used to identify rigid and floppy domains in 2D random truss lattices[29], but for general network structures, efficient algorithms do not yet exist. The dynamical matrix[30], which contains the connectivity information of the network, is a useful tool for linear response analysis, including the computation of shape changes that do not cost energy in truss[31] and granular[32] materials. A pressing question is how to extend these ideas to capture a broad range of nonlinear and large-deformation behaviours.

In parallel, research on the relationship between the microscale network structure and macroscopic material behaviour characterized the elastic properties of both naturally occurring[33,34] and conventionally synthesized materials[35,36]. This effort revealed distinct scaling relations across deformation regimes and led to the development of materials selection charts[33,37] for comprehensive assessment of cost versus performance. One outcome of this line of research was the realization that architected materials can achieve performance outside the property space occupied by ordinary materials[38]. The design of architected materials has been facilitated by topology optimization[39] — a computational approach that combines linear programming with finite-element analysis. Although this approach is not readily scalable to irregular metamaterials, it has assisted the optimization of regular and locally coupled materials[40,41].

This Perspective has two complementary goals: to show that irregular metamaterials can exhibit enhanced properties relative to regular ones and that a suitable network representation of such materials facilitates their description, analysis, prediction and design. Here, the term 'irregular' refers to systems that are not formed by repeated building blocks but that can still be highly organized, as is common in optimized structures. Irregular metamaterials thus include, but are not limited to, disordered materials characterized by random deviations from regularity. We distinguish between topological, geometrical and parametric irregularity. These three types of irregularity are naturally accounted for in network representations, and we present measures to quantify them. We explore two representative network models to illustrate and overcome the challenges associated with the generation of physical networks. This motivates us to discuss how machine learning can aid in the design of irregular metamaterial networks and how the networks themselves may undergo physical learning. Having established the potential of irregular metamaterial networks, we review how additive manufacturing techniques can be used to fabricate the proposed materials and highlight outstanding problems and opportunities for future research.

Metamaterial networks

A recurrent claim in network science has been that network structure influences — or even determines — function. For example, the percolation threshold in random networks is determined by the moments of the distribution of degrees[12] (that is, the distribution of the number of interactions per node), which underlie the well-established vanishing of the epidemic threshold in scale-free networks[42]. In the master stability formalism[12], the stability of network states is governed by the eigenvalues of the Laplacian matrix, which, in the context of synchronization, generally implies that synchronized behaviour is more strongly supported in networks with a localized spectrum of non-identically zero eigenvalues[43]. Similarly, because nodes tend to connect to others that are more highly connected than themselves[12], high-degree nodes disproportionately mediate dynamical processes in complex networks, shaping the speed and pathways of diffusion and influence[44].

Crucially, the connection between structure and function is believed to largely hold in materials too[35,36]. For example, because the allotropes of carbon are all made up of the same atoms, the dissimilar properties of diamond and graphite must emerge from the network structure, that is, the topology, geometry and nature of interactions. Conversely, the tetrahedral covalent network of diamond is also found in other ultra-hard materials with different elemental compositions, such as silicon carbide and carbon nitrides[45,46]. In the materials literature, the method of topology optimization formalizes the structure–function relationship through pixellated descriptions of the filled material volume[47,48]. This approach can programme preferred deformation modes known as compliant mechanisms by using optimization to determine where material elements should be deposited in the finite-element grid[49]. The architecture and nature of interactions in both ordinary materials and those constructed through topology optimization are constrained by the adjacency of chemical and physical bonds. This constraint limits the overall network structures to generally being locally coupled, whether or not they are ordered (as in the case of crystals), designed (as in the case of topology optimized structures) or disordered (as in amorphous solids). Moreover, the metamaterials literature has focused mainly on structures that are not only locally

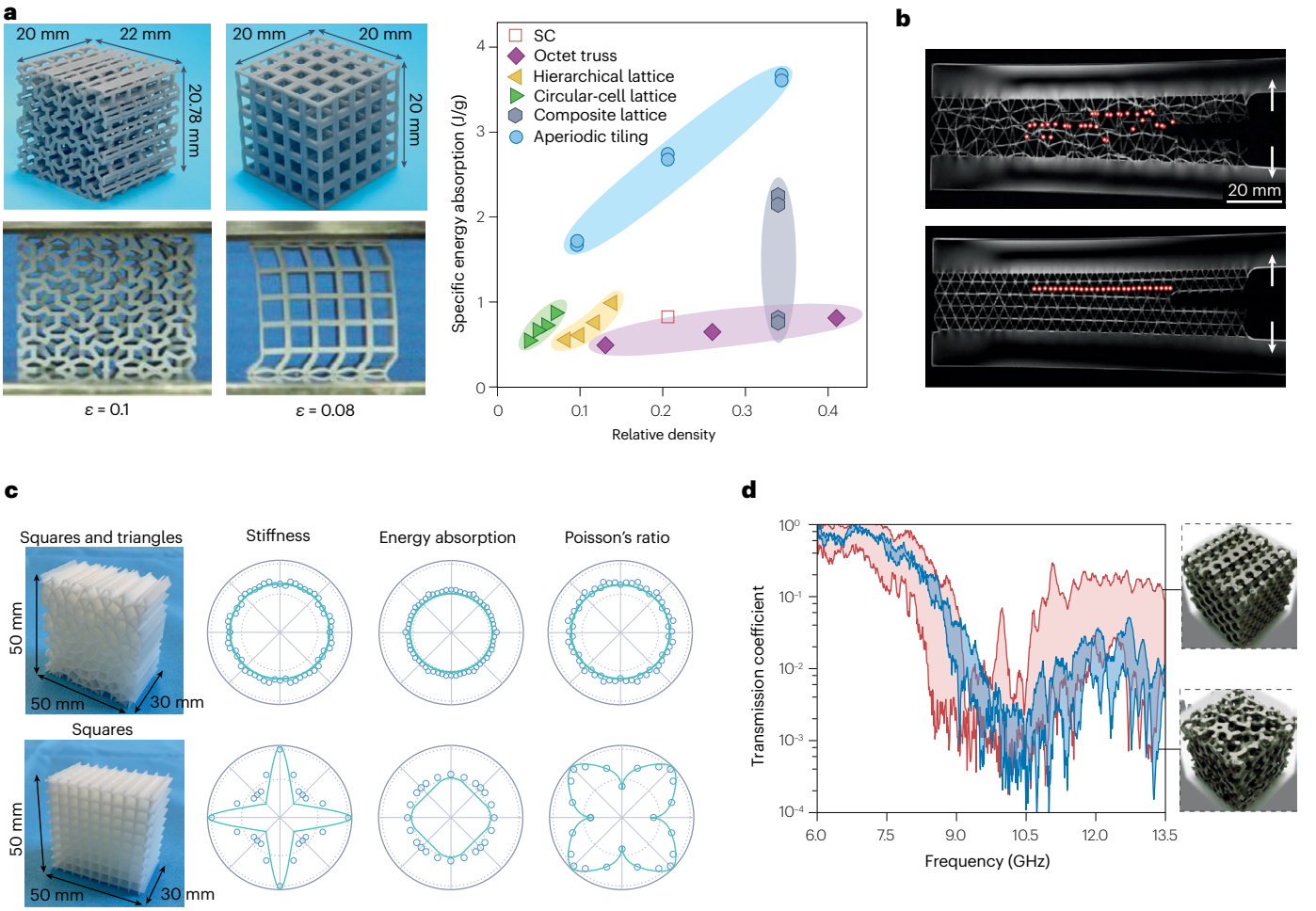

Fig. 1 | Examples of exceptional behaviour achieved by irregular metamaterials. a, Samples of aperiodic (top, left) and simple cubic (SC; top, centre) structures, their behaviour at approximately 10% strain (bottom, left and centre, respectively) and their specific energy absorption as a function of the fraction of the volume occupied by material (right). The aperiodic structure (strain $\varepsilon = 0.1$) exhibits more localized buckling compared with the SC structure ($\varepsilon = 0.08$), leading to a substantial increase in specific energy absorption at fixed density relative to other regular structures[170]. **b**, Fracture propagation (red dots) in an irregular truss structure (top) vs its regular counterpart (bottom) when the right side is pried apart (white arrows). The irregular structure deflects the crack tip, leading to a doubling of the fracture toughness[162]. **c**, Isotropy of the stiffness, specific energy absorption and Poisson's ratio for an aperiodic lattice of squares and triangles (top row) compared with the anisotropy of these characteristics for the square lattice (bottom row)[171]. Regular lattices necessarily have anisotropic off-axis responses and have markedly different properties when applied stresses are not aligned with the lattice vectors. **d**, Approximate isotropic light transmission behaviour of an irregular hyperuniform structure (blue; bottom, right) compared with the strongly anisotropic behaviour of the diamond lattice structure (red; top, right), in which the coloured area spans the range of minimum to maximum transmission coefficients at a given frequency across the three principal directions[172]. The minimum in transmission coefficient across all directions slightly above 10 GHz reflects that the material is substantially more opaque to photons at this frequency than at higher and lower frequencies. Panel **a** adapted with permission from ref. 170, Wiley. Panel **b** adapted from ref. 162, CC BY 4.0. Panel **c** adapted with permission from ref. 171, Elsevier. Panel **d** adapted from ref. 172, CC BY 4.0.

coupled but also largely regular. These constraints facilitate design by keeping the search space more tractable, but they restrict the range of new properties that can be explored.

Importantly, metamaterials are not inherently limited to local coupling and a nearly regular structure. Exploring more general networks can increase the space of possibilities, bringing about opportunities to realize new or enhanced properties. Although many properties of interest — including specific stiffness, specific strength and wave attenuation at selected frequencies — are achieved through periodic designs, research on neuromorphic metamaterials[50], nature-designed structures[51] (including those made of protein, cartilage and muscle[52]), damage-resistant topologies[53–55] and disordered auxetic systems[56] shows that substantial gains are possible by departing from regular and/or locally coupled network structures. Further advances in irregular metamaterials research have been inspired by naturally occurring disordered materials such as foams, glasses, granular materials and amorphous systems, as well as (irregular) polymers, biological tissues and animal-built structures. An important question for future research is how to comprehensively design and optimize metamaterials by systematically exploring a wide range of irregular networks.

We note that the same network structure can describe irregular granular, truss and plate materials (Fig. 2). The elements of the

underlying network are associated with material constituents of increasing complexity, which interact through points of contact in granular systems (Fig. 2a), through elastic beams in truss lattices (Fig. 2b) and through surfaces in plate materials (Fig. 2c). The properties of the underlying network (Fig. 2d), such as percolation and the eigenvalue spectrum, can inform material behaviour such as rigidity[57] and floppy modes[28]. Nevertheless, this network representation has limitations. First, the network was derived from the granular system in Fig. 2a and then used to generate the truss and plate materials in Fig. 2b,c and thus was not generated a priori based on desired material properties. Second, the description in Fig. 2d does not distinctively define the material and can correspond to vastly different outcomes, including but not limited to those shown in Fig. 2a–c. The network representation must be augmented with additional information to render a complete description of the material and to inform analysis and design.

Beyond irregular topology

Networks can be — and in other domains they generally are — irregular in their full scale[58] and may involve directed coupling[59]. A metamaterial designed with this structure would not have finite-size unit cells in the thermodynamic limit, may exhibit a divergent variance in the number of interactions per network node and could potentially undergo new types of phase transition owing to non-reciprocal interactions[60]. Traditional network models cannot be used to design such irregular metamaterials because, apart from the interaction strengths, they describe only the topology of the network. Metamaterials are embedded in the physical space, and a realistic account of their properties requires modelling both the geometry and the nature of their network elements.

Traditional network models

Some of the most widely used models in network science[11,12] are commonly visually represented as dots (nodes) connected by lines (edges) and expressed as matrices $A = (A_{ij})$, in which A_{ij} is the strength of the edge from node j to node i (Fig. 3a–d). The power of such models lies in their ability to capture essential properties that are frequently observed in real networks, including short node-to-node distances[61], skewed distribution of connections per node[62] and community structure[63], while facilitating the characterization of emergent phenomena for entire network ensembles[64]. Generalizations beyond static pairwise interactions of a single type have also been explored through models that account for higher-order[65,66], multilayer[67,68] and temporal interactions[69,70] (Fig. 3e–g). Notwithstanding their usefulness, all models in Fig. 3 are essentially limited to describing the topology of a system. Although there are physically embedded networks — such as power grids[16], social proximity networks[71], pedestrian flow networks[72] and the Internet[73] — that are meaningfully captured by variants of traditional network models[58], we argue below that the network modelling of metamaterials requires further extensions of network theory itself.

Types of irregularity

Research progress in irregular metamaterial networks requires a suitable definition and quantification of irregularity. Different types of

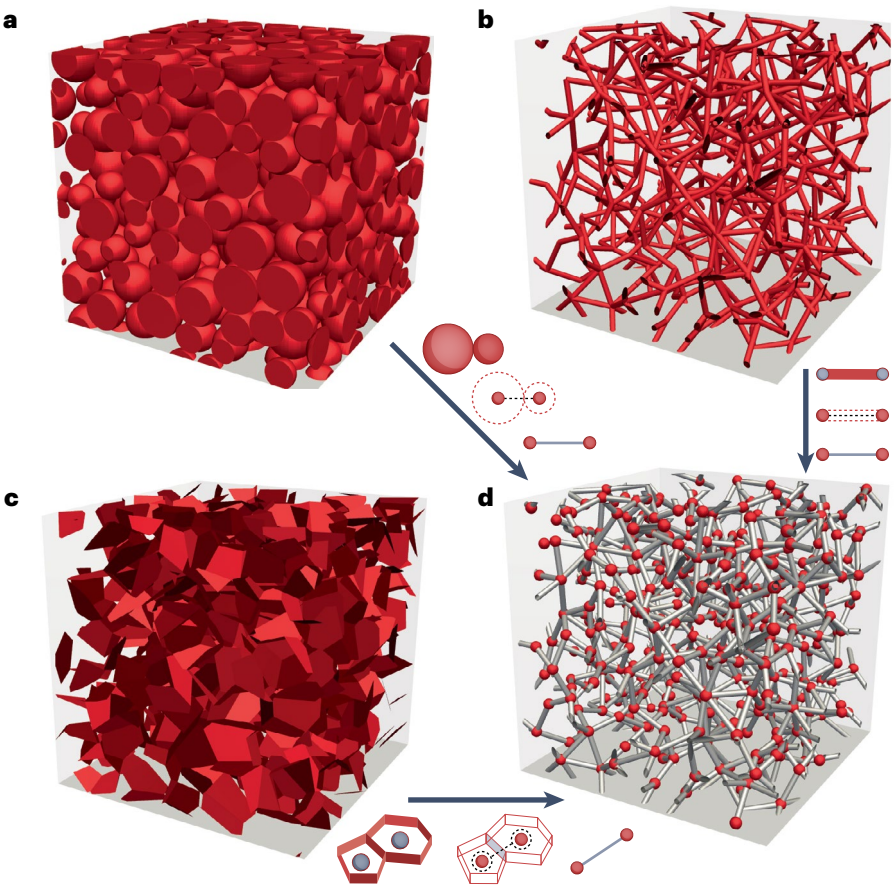

Fig. 2 | Metamaterials of different classes described by a common network structure. a–**c**, Irregular granular (panel **a**), truss (panel **b**) and plate (panel **c**) structures, corresponding to interactions of increasing dimension and complexity, respectively, represented by point contacts between grains, beams between truss nodes and surfaces between Voronoi cells. **d**, The underlying network, which is the same for all three structures. The arrows indicate the relationship between the material elements and the underlying network. Additional details on the network construction are provided in the Supplementary Information. Figure inspired by ref. 173.

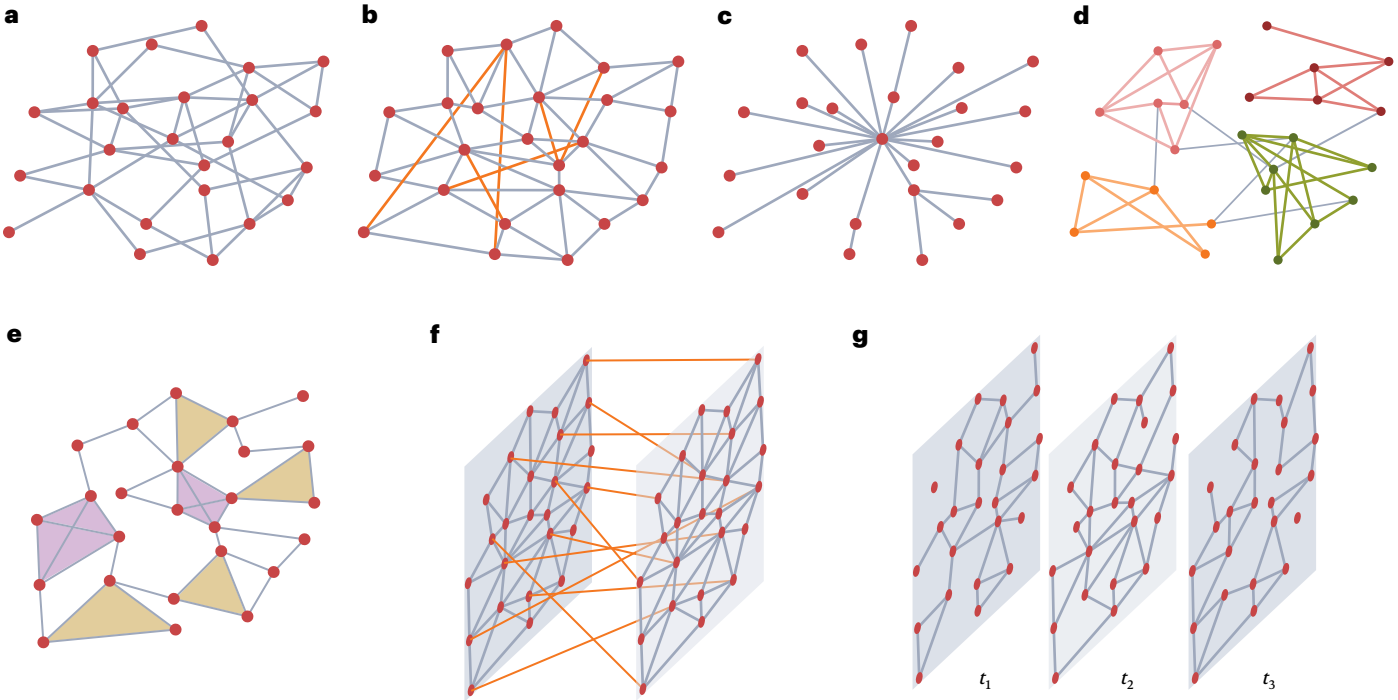

Fig. 3 | Irregular networks generated by purely topological models. **a**, Erdős–Rényi network, in which node pairs are connected by an edge with a given probability. **b**, Small-world network, generated through the rewiring of a fraction of edges (orange) in a triangulated lattice. **c**, Scale-free network, generated by randomly connecting nodes with a pre-assigned power-law distribution of the number of connections, leading to hub nodes with a large number of connections. **d**, Network with communities of densely connected nodes generated using the stochastic block model with four planted clusters. **e**–**g**, Generalized networks: higher-order networks with interactions involving more than two nodes (panel **e**), multilayer networks featuring different interaction types or systems (panel **f**) and temporal networks capturing time-varying connectivity (panel **g**).

network irregularity can be explored in the design of metamaterials, including topological, geometrical and parametric irregularities (see Supplementary Fig. 1). At the most fundamental level, topological irregularity concerns the form of the underlying graph with no reference to physical distances. This form of irregularity is important, for example, in determining percolation transitions[64]. Geometrical irregularity refers to how the size, shape and/or orientation of the network nodes and/or edges can vary unevenly in space. Parametric irregularity concerns node and edge properties not captured by topology and geometry. These properties define the nature of the network elements and can include mass density, composition, damping coefficients and elastic moduli, among others. By dividing the types of irregularity into these categories, we arrive at a natural conceptualization of irregular metamaterials that applies to both engineered and natural materials[74]. For all three categories, the irregularity can be localized (as for a defect), structured (as for gradients and holes) or statistically uniform across the entire network (as for uniformly random systems). The extent of irregularity generally depends on the scale at which the metamaterial is observed. As for other material network properties, this scale dependence can be quantified using persistent homology analysis[75].

Quantifying irregularity

The deviation of irregular metamaterials from regular patterns formed by repeating structures is reflected in the underlying network and its associated parameters. This deviation can be quantified by network symmetries, the configuration and information entropies, and fluctuations in the local volume fraction.

Network symmetries. Network symmetries can be defined in terms of the network's automorphism group[76] and its generalizations. The automorphism group is formed by all node permutations $i \to \pi(i)$ that leave the network unchanged. Structurally identical nodes are related by a permutation and belong to the same orbit of the automorphism group (symmetries can be defined similarly for edge permutations). The orbits form a partition of the network. Regular network structures have more symmetries than irregular ones, which can, in the most extreme cases, have no symmetry other than the identity. Network symmetries have been used to characterize network irregularity in other applications, including synchronization dynamics[77–79].

Configurational and information entropy. Entropy is a measure of disorder often used in dynamical contexts, but it can also quantify structural irregularity. In an ensemble of networks, each network corresponds to a configuration assigned a probability P_n of being observed. The configurational entropy[80] of the ensemble is proportional to the Gibbs entropy $S_G = -k_B \Sigma_n P_n \ln P_n$, in which k_B is the Boltzmann constant. A network ensemble consisting of one or only a few configurations, such as a lattice network, has a much lower entropy than an ensemble of random networks. The probabilities P_n depend on the details of how the ensemble is defined[81,82]. For example, random networks generated from a given degree sequence define a microcanonical ensemble in

which every network structure with the specified degrees has an equal probability. By contrast, the Erdős–Rényi model (Fig. 3a) defines a canonical ensemble, in which all network structures are possible but with a probability proportional to a network version of the Boltzmann factor.

Alternatively, irregularity can be measured by quantifying the amount of information needed to specify the structure of the system. The amount of information can be quantified by covering a realization of the material network with a fine grid in which grid boxes overlapping with the material are assigned 1 and empty boxes are assigned 0. The spatial organization can be captured, for example, by dividing the sequence of ones and zeros into blocks. The Shannon information entropy[83,84] can then be applied to this sequence of blocks to measure the information content in the structure. (A similar approach can be used to measure irregularity based on the presence and absence of entire edges in the network). The Shannon entropy is similar in form but different in content from the Gibbs entropy, as the former concerns the organization of an individual realization and the latter concerns the probability of observing different realizations. Once again, a repetitive structure is expected to require less information, and hence have a lower entropy, than an irregular one.

Local volume-fraction variance. The local volume-fraction variance is another quantity that can be used to measure structural irregularity. This quantity is the variance of the fraction of the volume occupied by the material within a ball of radius R as the ball's centre is varied[85]. For d-dimensional materials, the volume fraction often scales as $R^{-(d+\xi)}$. The parameter ξ contains information about the material's structural irregularity: $\xi = 1$ for lattices, $0 < \xi \leq 1$ for a range of disordered hyperuniform structures, $\xi = 0$ for uniform randomness and $-d < \xi < 0$ for anti-hyperuniform structures. This fluctuation-based characterization of irregularity captures long-range spatial correlations, which are relevant to the design of metamaterials[86].

Although the measures described above characterize irregularity in the material structure, they can be extended to account for (possibly continuous) parameter dependences, such as the elastic modulus. These measures can thus quantify not only topological irregularities but also geometrical and parametric ones, as well as combinations of the three.

Geometry-endowed network models

The first requirement for a metamaterial network is geometry, but therein lies the challenge: direct top–down attempts to incorporate geometry in existing generative models of irregular networks often lead to intersections and crossings of nodes and edges in the physical space. The prohibition of such overlaps is referred to as the volume exclusion constraint. Another requirement is that the edge distribution must decay with edge length. Owing to volume exclusion and resource limitations, an edge between two nodes should become less likely if the nodes are sufficiently far apart. This property is featured in several models of physically embedded networks, most notably in the description of synaptic connectomes[87,88] (but also in spatial network models that are not constrained by volume exclusion[89–94]).

By contrast with many other physically embedded network systems, such as microfluidics, brains, power grids and computer chips, mechanical metamaterials are not static within the relevant timescales. Thus, geometry-endowed network models need to be developed to satisfy the volume exclusion constraint not only in a fixed equilibrium state but also when stressed, strained, acoustically driven, heated and/or damaged. An emerging body of research in the network science community (Box 1) has begun to grapple with the effects of volume exclusion[24,25], physical edge entanglement[95–97] and physically extended nodes[98,99]. This line of research has two important frontiers: one considers the elastic behaviour of the nodes and edges while respecting volume exclusion under loading, and the second accounts for the cost of physical edges and nodes. The latter was considered in a work describing how the morphology of natural physical networks is driven by surface optimization[99]. In what follows, we present two network models that can incorporate the different types of irregularity, satisfy volume exclusion and account for the cost of the material network.

Network model with physical constraints

To appreciate the impact of geometry, we consider a simple geometric extension of the Erdős–Rényi model, which is representative of a broader ongoing initiative to develop physical network models that incorporate geometry into topological network designs. In its standard formulation, the Erdős–Rényi model is purely topological: each pair of nodes is connected independently with fixed probability p. We formulate a 3D geometric extension in which nodes are centred at randomly selected points in the unit cube with no more than one node within each voxel of a S^3 grid; nodes are balls and the edges are rods, both assumed to have radius $d \geq 0$; and an edge connects a pair of nodes (i,j) with probability $\min\{cr_{ij}^{-\alpha}, 1\}$, under periodic boundary conditions. Here, r_{ij} is the (Manhattan) distance between the nodes, $\alpha \geq 0$ is the decay exponent and $c > 0$ is a constant that assumes the role of p in the topological Erdős–Rényi model (Fig. 4a). This model can incorporate several previously considered concepts, such as the decay of the edge probability with distance[91,94,100], volume exclusion[24,25], edge entanglement[95] and percolation[92,94,101], into a single construction.

In the limit in which the radius of the edges and nodes is zero ($d = 0$), volume exclusion is automatically satisfied for any finite number of nodes, and all edges are placed independently of each other. Nevertheless, the average node degree at the percolation transition — at which a giant connected component forms — increases from 1 if the decay exponent α becomes sufficiently large. For example, if the number of nodes is $N = 6{,}250$ and the number of voxels per side of the principal volume is $S = 50$, the average degree at the percolation transition is larger than 1 for $\alpha \geq 2.5$, meaning that connected components consist of a larger number of shorter edges (Fig. 4b). The degree needed to obtain a single connected component with a fixed probability e^{-1} remains fixed at $\frac{1}{2}\ln N$, which is the same threshold as in the (purely topological) Erdős–Rényi model (see Supplementary Information for additional model details). The decay parameter α tunes the network to reach the connectivity transition with less material because the typical edge length shortens as α increases (Fig. 4c). If the system is subject to a non-affine straining, edge or node crossings can occur, and the fraction of edge crossings grows linearly with the maximum strain (Fig. 4d). If the edge (and node) thickness is non-negligible, overlaps occur with a frequency that grows linearly with d even in the absence of loading (Fig. 4e). Such violations of volume exclusion can be addressed by allowing edges to have curvature and/or by fusing overlapping sections. In the latter case, the nodes are no longer independent when $d > 0$.

Networks from adjacency-constrained tiling

As an approach that more directly incorporates the physical constraints above, we consider the recently introduced virtual growth model[102]. The building blocks are tiled randomly, and the short-range

Box 1 | Emerging models of physical networks

We comment on two growing classes of physical network models of relevance to metamaterials. The first class extends traditional network models by embedding nodes and edges in 3D space. Models within this class can describe long-range interactions and represent structures that satisfy volume exclusion even when edges and/or nodes have finite volume. In one model, edges of defined thickness are sequentially added between nodes until no more edges can satisfy volume exclusion[24,25]. The problem of satisfying edge volume exclusion is mapped onto the identification of independent sets of 'metagraphs'[25] (see the figure, panel **a**). Another model focuses on physical entanglement, in which nodes and edges embedded in space form knots[95] (see the figure, panel **b**). This model can relate the presence of knots to the behaviour of complex liquids[95,181,182], solids[183], gels[184] and other networks of intertwined fibres[52,185,186]. In a third model, the nodes are chain subnetworks that are grown on a defined grid until they run into another node, thus forming an edge[98] (see the figure, panel **c**).

The second class of physical network models uses Maxwell frames — rigid rods of a fixed length (edges) that connect at hinge joints (nodes) — to prescribe the motion of target nodes in response to the actuation of distant source nodes. Models within this class programme specific mechanical behaviours by tuning the existence and length of the (primarily short-range) interactions between nodes. An early model was used to design 2D and 3D frames that exhibit allostery, in which the target nodes move apart in response to the source nodes being pinched together[27] (see the figure, panel **d**). This model illustrates how, even in locally coupled networks, architected disorder can be used to programme nonlocal responses in metamaterials beyond those mediated by wave propagation[187]. Further work developed a model to place source nodes (blue) with a predetermined deformation to achieve desired deformation patterns for the target nodes (red) in a given network[26] (see the figure, panel **e**). A similar approach has been applied to compose networks consisting of a series of building blocks that achieve prespecified folding patterns[188] (see the figure, panel **f**).

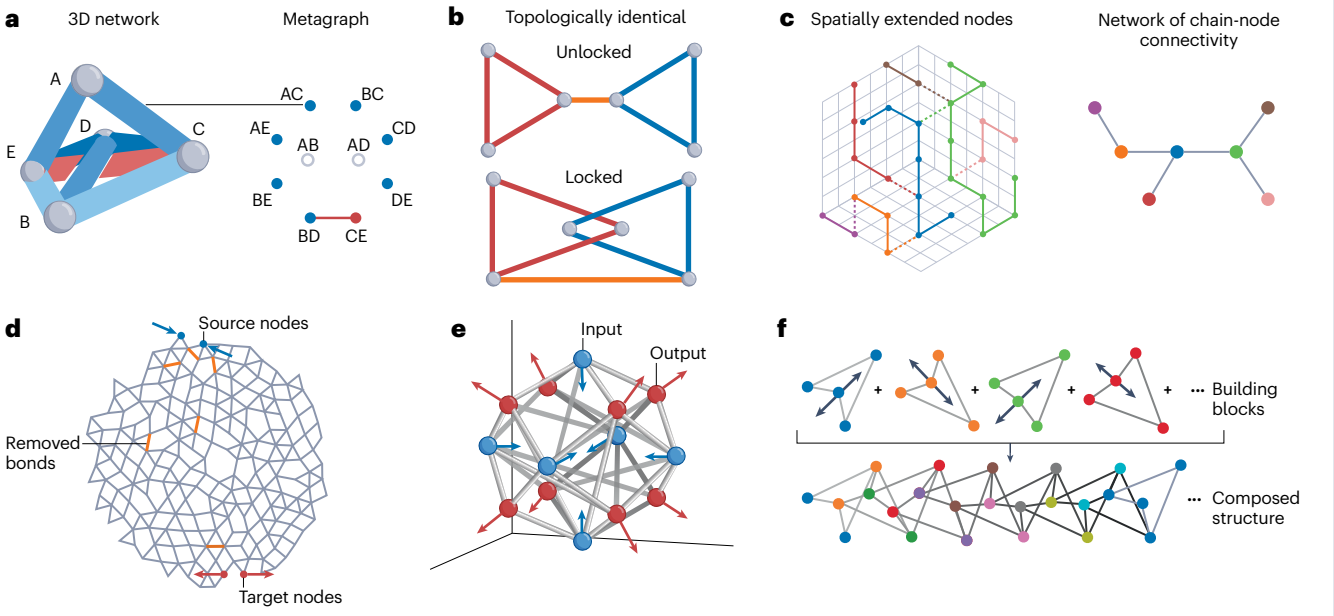

Panel **a** adapted from ref. 25, Springer Nature Limited. Panel **b** adapted from ref. 95, Springer Nature Limited. Panel **c** adapted from ref. 98, CC BY 4.0. Panel **d** adapted with permission from ref. 27, Proceedings of the National Academy of Sciences USA. Panel **e** adapted from ref. 26, Springer Nature Limited. Panel **f** adapted from ref. 188, CC BY 4.0.

interactions between adjacent blocks satisfy certain compatibility rules (Fig. 5). A key ingredient of the model is that each building block includes not only nodes and edge segments but also their embedding in 2D or 3D space. Given a set of building blocks and compatibility rules, the model is entirely parameterized by the assigned proportions of the different building blocks. Throughout the generation process, compatible blocks are added sequentially, mimicking nest design strategies adopted by insects that use predominantly local information[103]. This bottom-up approach systematically generates ensembles of emergent irregular networks with a complexity that is intermediate between regular lattices (consisting of repetitions of a single building block) and random networks (which do not include repeated patterns). Physical realization can be achieved through 3D printing (Fig. 5e,f).

The degree of correlation between nearby building blocks (Fig. 5b–d) affects the percolation and physical properties of the material[104] but is not properly captured by widely used topological and geometric descriptors such as the Minkowski functionals[105]. These

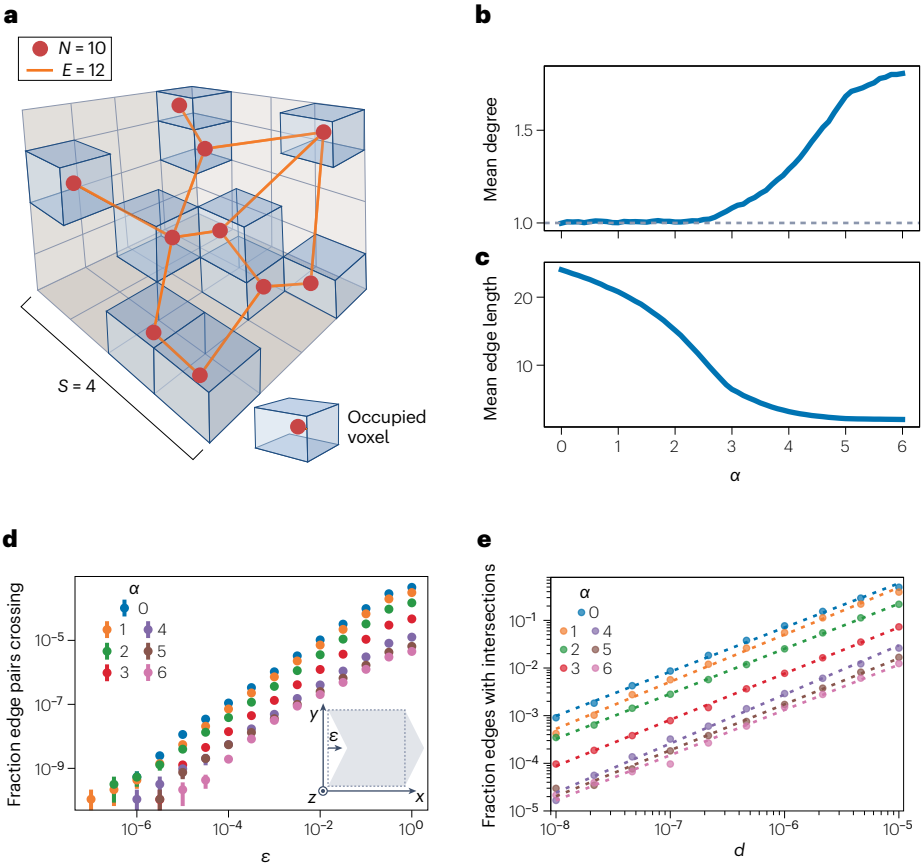

Fig. 4 | Geometric extension of the Erdős–Rényi model. a, Example network for $N = 10$ nodes, $E = 12$ edges and $S = 4$ voxels per side of the principal volume, in which at most one node can be placed randomly according to a uniform distribution in each voxel. **b**, Mean degree at the percolation transition as a function of the decay exponent α for edge radius $d = 0$, which has qualitatively similar behaviour to a 2D spatial network model[94]. The dashed line indicates the degree in the (topological) Erdős–Rényi model. **c**, Mean length of the edges for the networks in panel **b**. **d**, Fraction of edge crossings (relative to the total number of edge pairs) in a strained material for $d = 0$ as a function of the maximum strain ε (in units of voxel side lengths) for the profile shown in the inset. **e**, Fraction of edges violating the volume exclusion constraint as a function of d in the absence of loading ($\varepsilon = 0$). In panels **b**–**e**, $N = 6{,}250$ and $S = 50$; in panel **d**, error bars larger than the symbol denote the s.e.m.

functionals, which in two dimensions comprise the Euler characteristic, perimeter and area of the material structure, characterize the material size and shape additively: each Minkowski functional of the whole material is a function of the fraction of each type of building block and material connections formed between adjacent building blocks. Because additive descriptors ignore correlations, holistic network-based descriptors are needed to capture the nonadditive emergent properties of metamaterials, as further discussed below.

It is instructive to compare the two types of network model just mentioned. The geometric extension of the Erdős–Rényi model treats nodes and edges as the fundamental building blocks. It enables long-range interactions but requires an explicit treatment of volume exclusion. The virtual growth model, by contrast, adopts fundamental building blocks comprising nodes, edge stubs and empty space. This approach constrains long-range interactions but automatically enforces volume exclusion and can be realized through a local bottom-up tiling process. Both types of model permit tunable disorder in topology, geometry and other parameters. We also suggest that both types of model are amenable to being combined with topology optimization[39] because the network representation can match the mesoscopic structure of the constitutive elements, thereby facilitating scalable optimization by reducing the number of elements needed to accurately describe the material. Reducing the number of elements while maintaining a faithful material description is particularly helpful in computationally intensive nonconvex optimization[106,107].

Learning for metamaterial network design

From network models to deep neural networks

A major technical challenge faced in designing irregular metamaterials with specified properties is the lack of suitable methods (aside from specific simulation-driven optimization[40]) for structure–property mapping, particularly when the system undergoes phase transitions[108], the network connectivity changes over time[109], or frictional forces are non-negligible[110]. By formulating irregular metamaterials as networks, they can be represented in a format conducive to training graph neural networks (GNNs), a class of deep neural networks designed for graph-structured data, to infer the structure–property mapping or learn effective dynamical equations. The latter application translates an idea to GNNs that has been used in convolutional neural networks[111,112] (CNNs) through graph convolutional networks[113]. Unlike CNNs, GNNs naturally allow network data to serve as input and can be trained on networks that vary in size[114]. The network data include the network topology, network geometry and possibly other node and edge parameters (Box 2). Geometric symmetries can be accounted for by augmenting the training dataset with transformed configurations that have the same property labels or by embedding such symmetries in the neural network structure[115].

Deep neural networks have also been used to infer structural properties from material imaging data[116,117]. This application is often carried out using an unsupervised variational autoencoder (VAE) architecture, which is designed to uncover patterns in the material image by explicitly encoding the high-dimensional input data into a lower-dimensional

latent space via an 'encoder' neural network[118]. A 'property predictor' neural network is trained in a supervised manner using latent variables as input and the material properties of interest as supervisory signals. These material properties can then be extracted from the latent space. The inverse design proceeds by identifying points in the latent space that correspond to the desired properties. Selected points are decoded into structures by using the latent variables as an input to the encoder run in reverse. The VAE architecture is generally operated on inputs of fixed size[116,117,119], although it is possible to combine VAE architectures with GNNs to cope with inputs of variable sizes[120].

Applications of machine learning to analyse and design metamaterials are a rapidly developing research area. For example, GNNs have been applied to predict force chains[121] and particle rearrangements[122] in granular materials using networks in which nodes represent grains and edges represent grain contacts (Fig. 6a). Another application is the prediction of heat transfer and stiffness in shell metamaterials in which the shell surfaces are represented by truss networks that serve as inputs to the neural network model[123] (Fig. 6b). Machine learning has also been applied to predict nonlinear stiffness in truss metamaterials for which the network consists of a point set connected by edges[119,124] (Fig. 6c). In these examples, the machine learning model serves as an emulator for potentially computationally expensive finite-element calculations of homogenized properties. When finite-element calculations are inexpensive (for example, when the behaviours are well captured by the elasticity of the elements), direct simulation-based optimization can be preferred over neural network approaches[125,126].

GNNs have also proved useful to optimize force-directed layouts[127] and thus to assign geometry to abstract networks by embedding them in the physical space. Such layouts position nodes and edges to reduce overlaps between them. The process can be interpreted as identifying a hidden metric space, which is an underlying space wherein distances between nodes correlate with the probability that they are connected[128]. This approach offers a path to create physical networks with a balance of local and nonlocal interactions.

Physical network learning

Metamaterials can be recognized as physical networks, and such networks can be trained to learn a specific behaviour by optimizing their parameters. Although traditional machine learning is a software implementation inspired by brain network learning, many other natural physical networks, such as the protein network underlying embryo development[129], also undergo learning (Supplementary Fig. 2). A salient feature of 'physical network learning' is that it is generally decentralized in the sense that the update rules are informed by local information, which stands in contrast to the global update rules used in the training of neural network models[130,131]. Crucially, when used for the design of metamaterial networks, physical implementations of learning are expected to lead to the emergence of irregular edge and node parameters[132]. Indeed, the irregularity itself is the key to the solution of the inverse problem of creating a desired response to a perturbation[133]. Such problems have often been considered for static properties, but learning dynamical responses is a current frontier in metamaterials research[134]. Learning in irregular metamaterial networks can not only

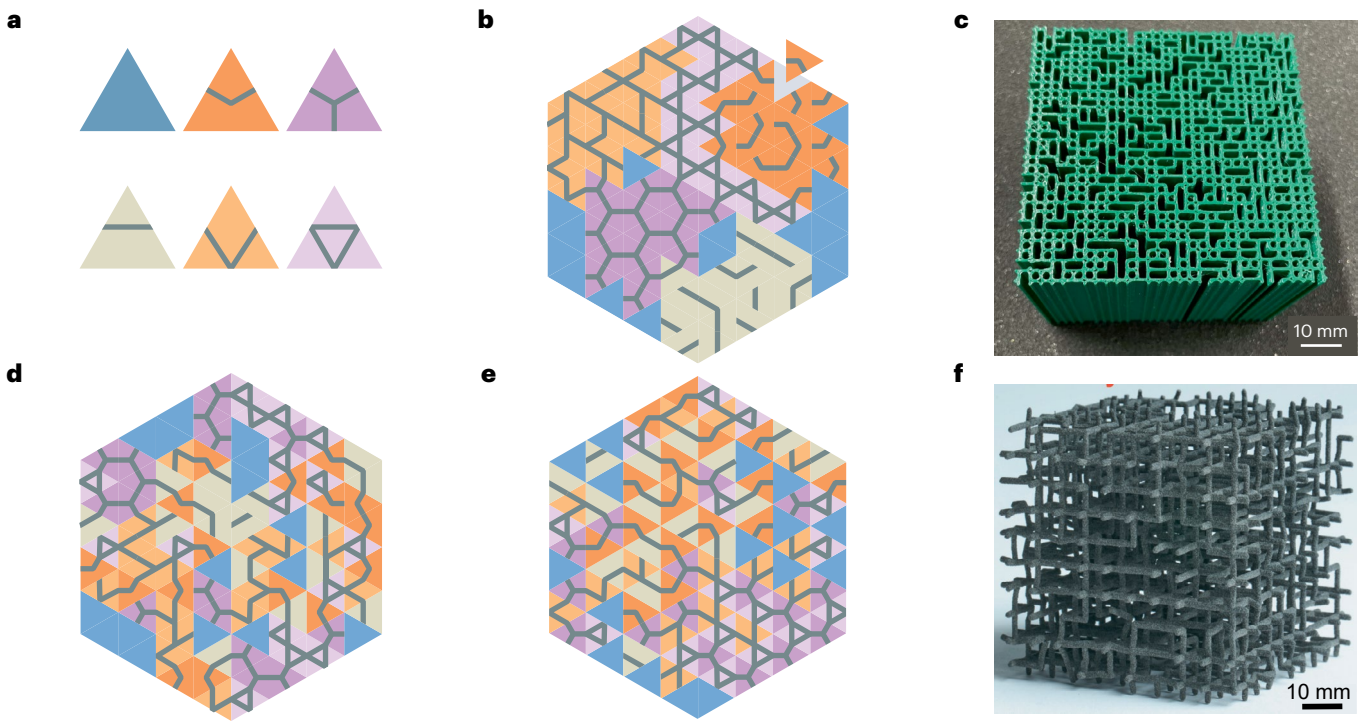

Fig. 5 | Network model and metamaterials based on virtual growth. **a**, Example building blocks in which edges (grey lines) and nodes (intersections between edges) are embedded in 2D space. **b**–**d**, Model realizations in which the connections between adjacent blocks are positively correlated (panel **b**), uncorrelated (panel **c**) and negatively correlated (panel **d**). These correlations determine how the same set of building blocks (with the proportion between different block types fixed) is arranged. **e**,**f**, 3D-printed metamaterial realizations of the model for designs with 2D square (panel **e**) and 3D cubic (panel **f**) building blocks. Panel **e**, image courtesy of Chelsea Fox. Panel **f** reprinted with permission from ref. 102, AAAS.

Box 2 | Graph neural networks for metamaterial design

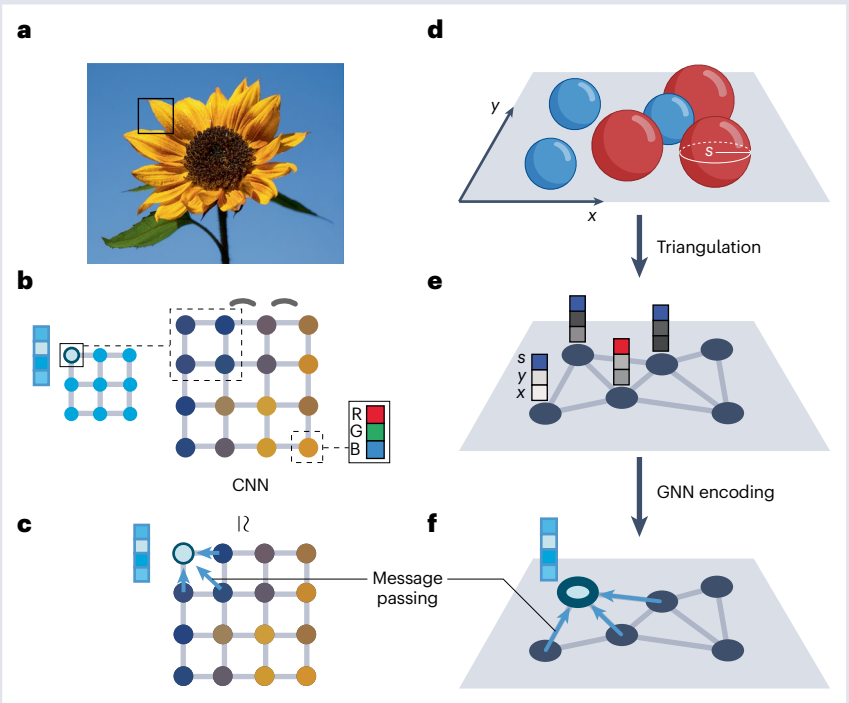

To understand how graph neural networks (GNNs) can be used in metamaterial design, we first review how convolutional neural networks (CNNs) process information in image classification[189]. CNNs construct a latent representation of an image (see the figure, panel **a**) by training a filter that takes a spatially weighted average of the red, green and blue (RGB) pixel values (see the figure, panel **b**). In this example, the filter is applied to the top left group of pixels (dashed box) and translated vertically and horizontally across the image to obtain the latent representation (blue grid), which is stored as a column vector (column of blue squares). This can be equivalently formulated as a message-passing operation on a regular lattice graph, whereby each node is a pixel and the (non-zero) filter weights are edges (see the figure, panel **c**). The underlying operation can be interpreted as a coarse-graining that extracts relevant local descriptors[158,159]. CNNs assume a fixed input size (proportional to the number of pixels) and a regular interaction structure (the lattice graph). Thus, they are generally designed for the analysis of continuum systems[111,112] — in which information between nodes is shared locally in space (such as image classification)[189] or time (for example, speech processing)[190]. GNNs adapt the message passing operation of CNNs to systems of varying input size and irregular connectivity[191] as required for irregular metamaterial networks.

In GNNs, message passing consists of applying a message function, an aggregation operator and an update function throughout all edges of the neural network. The message function generates an output from attributes associated with an edge and the nodes it connects. The aggregation function combines the output messages generated from all edges incident on a node. The update function performs the update of the node representation using the aggregated message output. After a specified number of iterations, the node representations are fed into a readout layer, which maps them to the desired prediction, such as global stiffness or localized failure.

Learning in GNNs involves training the weights in the message function, update function and readout layer[192]. Material data can be interpreted as a network, which is generally irregular. Using polydisperse granular media as an example (see the figure, panel **d**), the grains are nodes and their contacts are edges in this network (see the figure, panel **e**). The nodes can have multiple degrees of freedom, such as particle positions (x, y) and radii (s), which are incorporated into the network representation. Message passing is implemented on the whole network structure (see the figure, panel **f**) and the node representation (column of blue squares) evolves according to the state of its neighbours in the graph. Crucially, both the aggregation function and the readout layer are equivariant with respect to their inputs, meaning that they accept an arbitrary number of arguments and are invariant to argument permutations. This property enables the same GNN to be trained on networks of different sizes. Such variation in size is common in irregular metamaterial networks.

Panel **a**, credit: Moment/Anastasiia Voloshko/Getty. Panels **b**–**f**, image courtesy of Efe Gokmen.

facilitate the design of metamaterials with exceptional properties but also offer new platforms for hardware implementations of machine learning and artificial intelligence systems[135,136].

Scalability of manufacturing approaches

State-of-the-art and emerging approaches

The fabrication of metamaterials has traditionally relied on additive manufacturing (AM), which offers exceptional design freedom for creating architectures with a broad range of geometric complexity[137]. Commercial AM techniques have enabled the realization of large-scale periodic metamaterials in diverse material systems: polymers through stereolithography[138] or fusion-based techniques[139], ceramics through binder jetting or direct ink writing[140], and metals through laser powder bed fusion[141]. These methods have become standard in the field owing to their reliability and scalability for macro-structured designs.

However, many of the most impactful metamaterial functionalities — particularly in optics, electronics and mechanics — require architectures with nanoscale or sub-micrometre features. Optical and electronic metamaterials often exploit unit-cell dimensions of the order of the wavelength of light to achieve tailored electromagnetic responses[142]. Similarly, mechanical metamaterials can harness nanoscale architectural features to enable ceramic constituents to approach their theoretical strength by suppressing flaw sensitivity and crack propagation[143]. These functionalities motivate the development

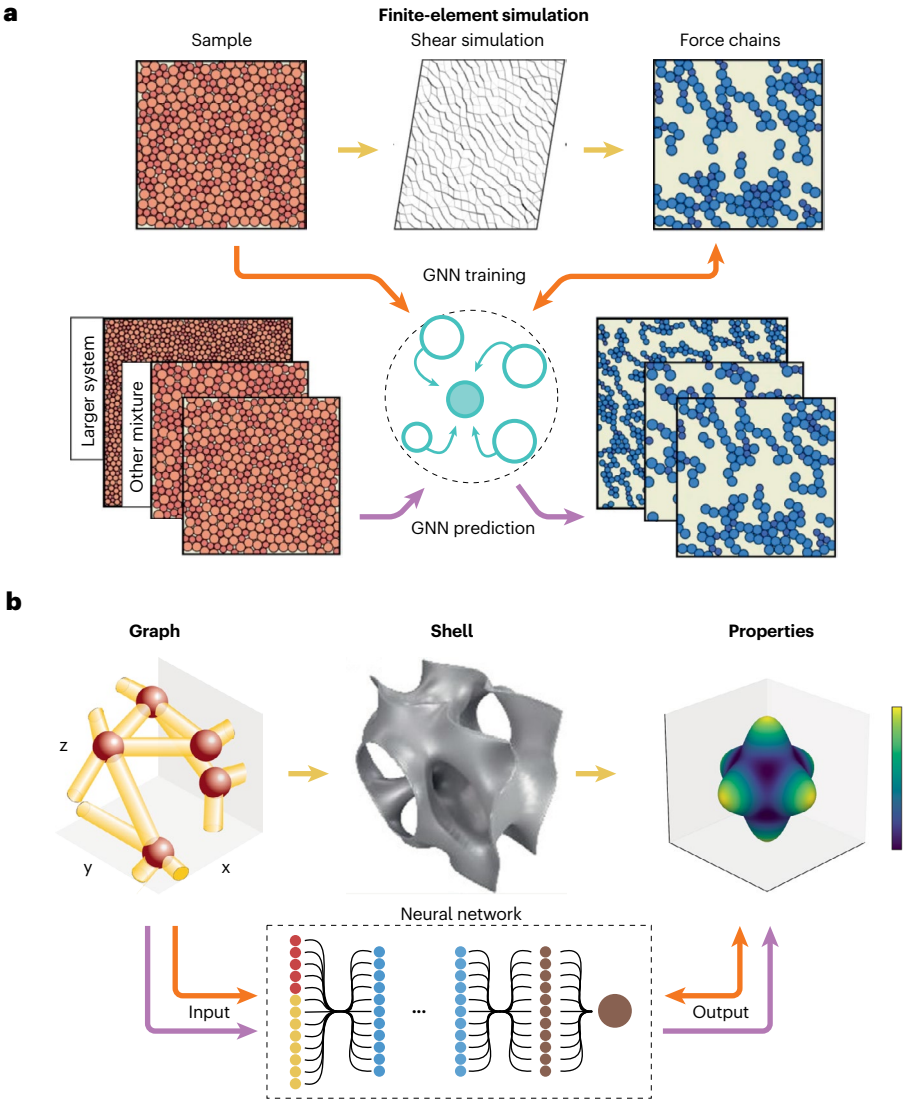

Fig. 6 | Neural networks for metamaterial analysis and design. a, Prediction of force chains in jammed packings of grains using a graph neural network (GNN; bottom centre) trained on material behaviour derived from finite-element simulations[121]. In all panels, yellow arrows denote (computationally expensive) simulation of material behaviour to extract the relevant properties. These properties form the supervisory signal for GNN training (orange arrows), which yields a model that can be used to design metamaterials by efficiently mapping material microstructure to macroscopic properties (purple arrows). **b**, Graph representation of shell metamaterials used to train GNN-based structure–property models[123]. **c**, Variational autoencoder framework to design truss-based metamaterials with tailored nonlinear behaviours trained on network topology and geometry[119]. Panel **a** adapted from ref. 121, CC BY 4.0. Panel **b** adapted from ref. 123, CC BY 4.0. Panel **c** adapted from ref. 119, CC BY 4.0.

of manufacturing strategies that produce macroscale samples from components of nanoscale resolution.

At present, two-photon polymerization direct laser writing (2pp-DLW) offers the highest spatial resolution available[144], and although historically confined to photosensitive polymers, its applicability has been expanded by advances in material conversion strategies. Techniques such as atomic layer deposition, pyrolysis, electroless deposition, electrodeposition and ion infiltration followed by thermal processing have enabled the transformation of printed polymer scaffolds into ceramics[143], metals[145], composites[146] and even glasses[147]. These methods have produced metamaterials with record-breaking strength-to-weight ratios[3] and new optical properties[147].

To overcome the inherent limitations of 2pp-DLW in terms of scalability, several promising developments have emerged. Projection microscale lithography enables faster fabrication of complex polymeric lattices over larger volumes[148], whereas new wide-area parallel direct laser writing systems are pushing the boundaries of high-throughput nanoscale printing. Techniques that can fabricate structural components at the metre scale generally have resolutions of the order of several millimetres to centimetres (for example, cold spray and wire-arc AM), whereas processes that enable architectural features at the sub-microscale (such as 2pp-DLW) are generally limited to sample sizes of a few millimetres (at least along two directions). Ultimately, all AM technologies inherently couple resolution and sample size, necessitating the development of new approaches based on self-assembly of the metamaterial from precursor components (Fig. 7).

Self-assembly approaches to enhance scalability

A fundamentally different emerging route to scalable metamaterial manufacturing leverages self-assembly followed by material conversion (Fig. 7). For example, phase separation in bi-continuous interfacially jammed emulsion gels (bijels) and block copolymers has been used

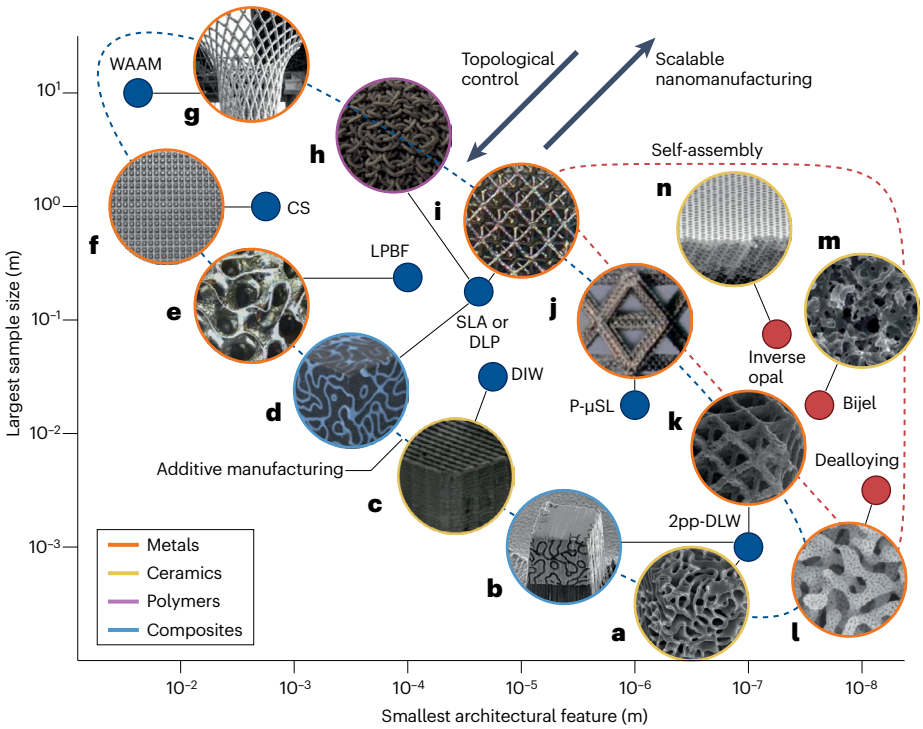

Fig. 7 | Inverse relationship between scale and resolution across fabrication techniques. a–n, Additive manufacturing (AM) technologies (blue dots) and self-assembly processes (red dots) can be used to fabricate periodic and disordered metamaterials of various constituent classes, including metals, ceramics, polymers and composites. The vertical axes indicate the maximal size of samples created by the technique, and the horizontal axis indicates the size of the smallest architectural feature in the material. The examples shown here are a carbon spinodal nanolattice[143] (panel **a**), carbon–nickel interpenetrating phase nanocomposite[146] (panel **b**), ceramic woodpile structure[140] (panel **c**), polymeric interpenetrating phase composite[150] (panel **d**), medium entropy alloy gyroid metamaterial[174] (panel **e**), 2D array of aluminium heat sink fins[175] (panel **f**), aluminium architected structure[176] (panel **g**), polymeric polycatenated architected material[138] (panel **h**), metallic microlattice[177] (panel **i**), multiscale metallic metamaterial[178] (panel **j**), metallic nanolattice[145] (panel **k**), hierarchical gold spinodal nanostructure[179] (panel **l**), graphene spinodal shell metamaterial from a bijel (bi-continuous interfacially jammed emulsion gel)[149] (panel **m**) and a ceramic inverse opal structure[180] (panel **n**). The state-of-the-art methods used to produce these materials include two-photon polymerization direct laser writing (2pp-DLW), projection micro-stereolithography (P-μSL), direct ink writing (DIW), stereolithography (SLA), digital light processing (DLP), laser powder bed fusion (LPBF), cold spray (CS) and wire arc AM (WAAM). Self-assembly methods such as inverse opal, bijel and dealloying represent one path towards scalable manufacturing while retaining the ability to fabricate sub-micrometre architectural features. Panel **a** reprinted with permission from ref. 143, Wiley. Panel **b** adapted with permission from ref. 146, AAAS. Panel **c** reprinted from ref. 140, CC BY 4.0. Panel **d** reprinted with permission from ref. 150, Elsevier. Panel **e** reprinted with permission from ref. 174, AAAS. Panel **f** reprinted with permission from ref. 175, Elsevier. Panel **g** reprinted with permission from ref. 176, Elsevier. Panel **h** reprinted with permission from ref. 138, AAAS. Panel **i** reprinted from ref. 177, Springer Nature Limited. Panel **j** reprinted from ref. 178, Springer Nature Limited. Panel **k** reprinted from ref. 145, CC BY 4.0. Panel **l** reprinted with permission from ref. 179, AAAS. Panel **m** reprinted with permission from ref. 149, RSC. Panel **n** reprinted with permission from ref. 180, Proceedings of the National Academy of Sciences USA.

to template ceramic shell lattices with spinodal topologies, which are irregular yet structurally robust architectures[149]. Pushing these technologies to larger scales and improving the ability to tune the degree of topological disorder are frontier areas of research.

Cutting-edge self-assembly techniques can yield structures with sub-micrometre wall thicknesses and sizes that extend to the centimetre or even metre scale (Fig. 7). Despite being initially viewed as a drawback, the irregularity inherent to self-assembled structures has since been recognized as advantageous, particularly in mechanical applications in which it promotes failure delocalization and enhanced energy absorption under dynamic loading[150].

As new disordered metamaterial architectures begin to emerge from network theory-driven design paradigms — whether truss based, shell based or particle based — they bring with them distinct challenges and opportunities for fabrication. One key challenge is to generate architectures with a highly tunable, application-specific type and degree of disorder. For structures in which control needs to be extended all the way down to nanometre scales, a particularly compelling research direction lies in tailoring the thermodynamics and kinetics of self-assembly processes. At macroscopic length scales, traditional techniques based on AM will remain distinctively capable for realizing disordered structures with exquisite control. New hybrid approaches could combine structuring by self-assembly at the smallest scales with AM at larger scales to exploit the advantages of each technique.

Challenges and opportunities

Irregular metamaterials have a larger parameter space than regular ones. Because regular is a limiting case of irregular, the optimum of a material property in the irregular case is at least as good as, but often superior to, that achievable in regular designs. The key challenge in exploring irregular designs is to circumvent the combinatorial explosion of the search space typical of such problems. Regular metamaterials are built from repetitive structures, often requiring the specification of only a single unit cell, whereas irregular metamaterials require the specification of macroscopic portions — or even the entirety — of the system. The macroscopic portions can be naturally represented as a network. Adopting a network perspective has enabled the design of materials with unusual properties such as solid-like and fluid-like behaviour in the same material[138], tunable isotropic negative Poisson's ratio[151] and enhanced resistance to damage[150] (Fig. 8). In the first example, the initial structure derives from a crystalline network, but dynamical relaxation of the (polycatenated) units introduces irregularity (Fig. 8a). The second example conceives the material as a truss network of stiff struts with flexible nodes and minimizes the Poisson's ratio by tuning the geometric locations of the nodes (Fig. 8b). The last example demonstrates the distinct damage tolerance of spinodal shells as they avoid stress concentration (Fig. 8c), in which networks can be used both to skeletonize the shell and to describe the percolation of force chains through the material.

Leveraging a network representation is advantageous first and foremost because, all else being equal, the structure (that is, the network) determines function. Because networks provide a faithful representation of structure, they can facilitate the design, optimization and analysis of metamaterials with desirable properties.

Forward problems

A common goal in metamaterials is to characterize the material properties using structural descriptors. Metamaterials exhibit nonadditive, emergent properties that arise from the interactions between building blocks. Because additive descriptors — such as Minkowski functionals — cannot account for correlations, there is a need for holistic descriptors that account for the properties of the material at all scales. Holistic descriptors based on suitable network representations can characterize system-wide patterns arising as the design parameters of the material are varied. Such descriptors could facilitate, for example, optimization of the stiffness and toughness of metamaterials without increasing their weight — both desired properties for aerospace applications — by exploring the ensemble of possible irregular configurations. Network descriptors can also assist dimensionality reduction without discarding key information about the interactions and correlations that ultimately govern the macroscopic behaviour of a metamaterial. For example, material rigidity can be characterized via the spatial inversion symmetry[152], as well as via an eigenvalue of a dynamical matrix[153] — nonadditive descriptors representing the underlying network — circumventing the more involved calculation based on Maxwell constraint count (and the associated determination of the null spaces of the compatibility and equilibrium matrices[28]). Once such a network descriptor has been identified, its application to the material properties constitutes a forward problem[131], in which predictions follow from the specified system.

Inverse–forward hybrid problems

Network modelling is well suited to the prediction of material behaviour or properties using a simplified representation rather than the complete physical description. Such simplified representations enable the integration of property prediction (forward problem) with the efficient search of material designs with desired properties (inverse problem). For example, the stress concentration that leads to material failure can be mapped to the problem of identifying communities of densely connected nodes that are sparsely connected with each other in the underlying network — a network concept previously applied to characterize material structure[154]. Such communities can be identified using community detection algorithms that partition networks based on edge betweenness centrality, which have been developed for arbitrary networks[12]. Edge betweenness centrality is the fraction of the number of shortest paths between pairs of nodes in the network that pass through a given edge, and is thus a measure of the edge's importance in connecting different parts of the network. Communities are revealed by sequentially removing the edges with the largest betweenness centrality, recalculating the betweenness after each removal[63]. A similar calculation can predict the sequence of bond breaking (and thus the most critical network components) when a metamaterial network is loaded[155]. This is the case because, in a material network, the edges between communities are expected to concentrate stress. In addition to its computational advantages, this modelling approach illuminates the relationship between a material's internal structural organization and its failure pathway — insight that is not immediate from direct finite-element simulations.

Analogous network-based surrogate prediction approaches have achieved remarkable success in biomedical[156] and sociotechnological[157] systems. A promising frontier in irregular metamaterials research is thus to develop such approaches to enable accurate predictions without recourse to exhaustive direct (for example, finite-element or molecular dynamics) simulations, which can be impractical, as is often the case when the deformations of a material are large, the structural topology is dynamic and friction is non-negligible.

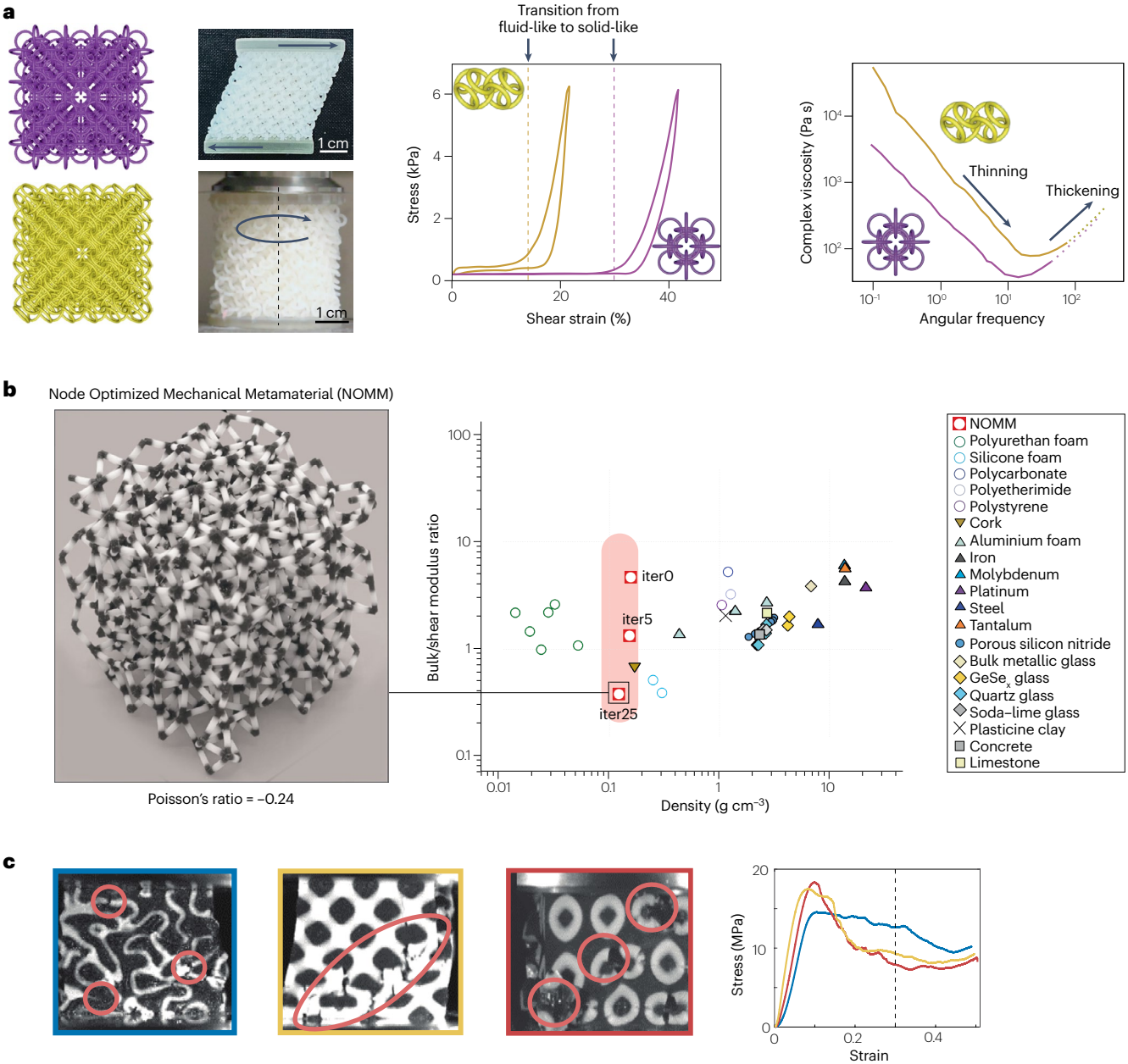

Fig. 8 | Irregular metamaterials whose unusual properties are governed by their underlying network. a, Polycatenated metamaterials (left images) exhibiting both solid-like and fluid-like behaviour under shear (top right image and left plot), as well as shear thinning and shear thickening under torsion (bottom right image and right plot)[138]. **b**, Truss metamaterial (left image) with a three-dimensional isotropic negative Poisson's ratio, which can be tuned by adjusting the locations of the truss intersections to decrease the ratio of the bulk and shear moduli (right plot, red shade)[151]. **c**, A two-phase composite spinodal shell metamaterial (left image) with increased energy absorption and damage resistance compared with an octet lattice (middle image) and a Schwarz-Primitive shell (right image). The enhanced properties can be seen through the reduction of material failure (red circles) at 30% strain (right plot, dashed line) and the extended stress-strain plateau (right plot, colour coded by the material image outlines)[150]. The irregularity in the materials in panels **b** and **c** is designed, whereas in panel **a**, the irregularity is induced by gravitational relaxation. Panel **a** adapted with permission from ref. 138, AAAS. Panel **b** adapted with permission from ref. 151, CC BY 4.0. Panel **c** adapted from ref. 150, Elsevier.

Inverse problems

The overarching goal in exploring a larger space of metamaterial structures is to design materials with desired properties and responses, including unprecedented ones. Network representations are distinctively suited to serve as a bridge to the incorporation of data and/or simulations into machine learning models based on GNNs. Such models yield a mapping from network structure to material properties, which can be inverted to obtain network structures that achieve the desired

properties. Having a network as an output is advantageous because the network abstraction is sufficiently flexible to incorporate a wide range of material structures of varying size and even composition when training the GNNs on different samples. GNN training involves recursive message passing on the underlying network: the learned message functions encode how local interactions are aggregated and propagated across network neighbourhoods so that local structural behaviour can influence properties across the entire material[158,159]. GNNs can naturally leverage network structure in the optimization of properties, such as fracture toughness, that are otherwise hard to calculate.

Synergies enabled by irregular networks

The advantages of irregular over regular metamaterials — and of representing irregular materials as networks — can be further appreciated by considering the effectiveness of artificial neural networks in machine learning. As in the case of neural networks, irregularity in materials expands the parameter space, enabling the representation of a wider range of possible behaviours. In both cases, optimization results in parameters that are irregular but not random. This is where another crucial advantage of the network representation (and its combination with GNNs) arises: it transforms irregular data into structured data that preserve correlations and suppress irrelevant variations, thereby facilitating interpretability, dimensionality reduction and generalization. This power can lead to advances on multiple fronts.

The expanded design space inherent to irregular metamaterial networks can lead to advances on multiple fronts, including multifunctionality, programmability, performance with robustness, multistability, inelastic behaviours and extreme or unprecedented properties. In particular, the resulting increased number of control inputs opens the possibility of systematically encoding multiple disparate or competing[2] properties within the same material. By the same principle, irregular metamaterial networks enable the programming[160] and reprogramming[161] of distinct responses to specific external stimuli, thus creating opportunities for dynamically tunable, modulable, reconfigurable and adaptive metamaterials. A major goal is to realize desirable functional properties in combination with robustness to ageing and failure[162,163]. The structure–property mapping of irregular metamaterial networks supports the simultaneous pursuit of both functional performance and robustness. Metamaterials based on irregular networks can be designed to exhibit multiple stable states with target properties, which in turn can lead to distinct nonlinear inelastic responses — such as negative compressibility transitions[108] — that are absent in monostable systems. Ultimately, an enlarged property space produces a structure–property mapping that is more complex, higher dimensional and harder to explore but also richer in potential functionalities[164].

It is thus clear that irregular network-based designs are advantageous not only for enhancing specific functions, such as energy dissipation, but also for improving robustness against localized failures. Broader exploitation of irregular metamaterial networks holds the potential to advance emerging areas, including topological, transduction, neuromorphic, active, biocompatible, microfluidic, space–time and quantum metamaterials, among others. At the same time, challenges such as managing the combinatorial explosion of parameters, training machine learning models with limited data and developing theory-guided approaches all highlight the value of a network-theoretic formulation.

Final remarks

A metamaterial network comprises topology, geometry and the properties of the network components, which are generally interdependent. For example, specific topological features emerge as a consequence of the spatially embedded nature of these networks, as illustrated in our geometric extension of the Erdős–Rényi model and observed in empirical physical networks[165,166]. This property of physical networks transcends metamaterials and architected materials[167], as exemplified by the suggestion that the network organization of the human brain itself might be strongly influenced by geometric constraints[168,169]. Previous research has shown the importance of network concepts in designing new metamaterial behaviour[108], in modelling coordinated motion of connected material parts[26] and hierarchical structural organization[98], and in characterizing the impact of geometric structure[25,95]. The field is now primed to develop a comprehensive network theory for systematically studying the space of irregular metamaterials with unprecedented properties.

Published online: 03 July 2026

References

1. Kadic, M., Milton, G. W., van Hecke, M. & Wegener, M. 3D metamaterials. *Nat. Rev. Phys.* **1**, 198–210 (2019).
2. Zheng, X. et al. Ultralight, ultrastiff mechanical metamaterials. *Science* **344**, 1373–1377 (2014).
   This article describes the use of projection micro-stereolithography to fabricate stretch-dominated microlattices with exceptionally high stiffness-to-weight ratios.
3. Crook, C. et al. Plate-nanolattices at the theoretical limit of stiffness and strength. *Nat. Commun.* **11**, 1579 (2020).
4. Smith, D. R., Pendry, J. B. & Wiltshire, M. C. K. Metamaterials and negative refractive index. *Science* **305**, 788–792 (2004).
5. Bertoldi, K., Reis, P. M., Willshaw, S. & Mullin, T. Negative Poisson's ratio behavior induced by an elastic instability. *Adv. Mater.* **22**, 361–366 (2010).
6. Lakes, R. S. Negative-Poisson's-ratio materials: auxetic solids. *Annu. Rev. Mater. Res.* **47**, 63–81 (2017).
   This review explores how mesoscale structures of varying degrees of irregularity expand the possible material behaviours using auxeticity as an example.
7. Guenneau, S., Movchan, A., Pétursson, G. & Ramakrishna, S. A. Acoustic metamaterials for sound focusing and confinement. *New J. Phys.* **9**, 399 (2007).
8. Cummer, S. A., Christensen, J. & Alù, A. Controlling sound with acoustic metamaterials. *Nat. Rev. Mater.* **1**, 16001 (2016).
9. Maxwell, J. C. X. L. V. On reciprocal figures and diagrams of forces. *Lond. Edinb. Dublin Philos. Mag. J. Sci.* **27**, 250–261 (1864).
10. Bollobás, B. *Random Graphs* (Cambridge Univ. Press, 2001).
11. Albert, R. & Barabási, A. L. Statistical mechanics of complex networks. *Rev. Mod. Phys.* **74**, 47–97 (2002).
12. Newman, M. *Networks* (Oxford Univ. Press, 2018).
13. Cook, S. J. et al. Whole-animal connectomes of both *Caenorhabditis elegans* sexes. *Nature* **571**, 63–71 (2019).
14. Dorkenwald, S. et al. Neuronal wiring diagram of an adult brain. *Nature* **634**, 124–138 (2024).
15. Piazza, B., Barabási, D. L., Menichetti, G., Ferreira Castro, A. & Barabási, A.-L. Physical network constraints define the multiplicative architecture of the brain's connectome. Preprint at *bioRxiv* https://doi.org/10.1101/2025.02.27.640551 (2025).
16. Yang, Y., Nishikawa, T. & Motter, A. E. Small vulnerable sets determine large network cascades in power grids. *Science* **358**, eaan3184 (2017).
17. Kleinberg, J. The convergence of social and technological networks. *Commun. ACM* **51**, 66–72 (2008).
18. Aral, S. & Walker, D. Identifying influential and susceptible members of social networks. *Science* **337**, 337–341 (2012).
19. Vespignani, A. et al. Modelling COVID-19. *Nat. Rev. Phys.* **2**, 279–281 (2020).
20. Arenas, A., Gómez-Gardeñes, J., Granell, C. & Soriano-Paños, D. Epidemic spreading: tailored models for COVID-19. *Europhys. News* **51**, 38–40 (2020).
21. Patwardhan, S., Rao, V. K., Fortunato, S. & Radicchi, F. Epidemic spreading in group-structured populations. *Phys. Rev. X* **13**, 041054 (2023).
22. Mocanu, D. C. et al. Scalable training of artificial neural networks with adaptive sparse connectivity inspired by network science. *Nat. Commun.* **9**, 2383 (2018).
23. Jankowski, R., Radicchi, F., Serrano, M. Á, Boguñá, M. & Fortunato, S. Task complexity shapes internal representations and robustness in neural networks. *Mach. Learn. Sci. Technol.* **7**, 025045 (2026).
24. Dehmamy, N., Milanlouei, S. & Barabási, A. L. A structural transition in physical networks. *Nature* **563**, 676–680 (2018).
25. Pósfai, M. et al. Impact of physicality on network structure. *Nat. Phys.* **20**, 142–149 (2024).
    This article is among the first to develop a statistical network model that contends with volume exclusion.
26. Kim, J. Z., Lu, Z., Strogatz, S. H. & Bassett, D. S. Conformational control of mechanical networks. *Nat. Phys.* **15**, 714–720 (2019).
    This article presents a simple method to design conformational changes in networks of freely rotating struts with fixed length.

27. Rocks, J. W. et al. Designing allostery-inspired response in mechanical networks. *Proc. Natl Acad. Sci. USA* **114**, 2520–2525 (2017).
28. Mao, X. & Lubensky, T. C. Maxwell lattices and topological mechanics. *Annu. Rev. Condens. Matter Phys.* **9**, 413–433 (2018).
29. Jacobs, D. J. & Thorpe, M. F. Generic rigidity percolation - the pebble game. *Phys. Rev. Lett.* **75**, 4051–4054 (1995).
30. Tanguy, A., Wittmer, J. P., Leonforte, F. & Barrat, J. L. Continuum limit of amorphous elastic bodies: a finite-size study of low-frequency harmonic vibrations. *Phys. Rev. B* **66**, 174205 (2002).
31. Ellenbroek, W. G., Zeravcic, Z., van Saarloos, W. & van Hecke, M. Non-affine response: jammed packings vs. spring networks. *Europhys. Lett.* **87**, 34004 (2009).
32. Ellenbroek, W. G., Somfai, E., van Hecke, M. & van Saarloos, W. Critical scaling in linear response of frictionless granular packings near jamming. *Phys. Rev. Lett.* **97**, 258001 (2006).
33. Wegst, U. G. K. & Ashby, M. F. The mechanical efficiency of natural materials. *Philos. Mag.* **84**, 2167–2186 (2004).
34. Gibson, L. J., Ashby, M. F., Karam, G. N., Wegst, U. & Shercliff, H. R. The mechanical properties of natural materials. II. Microstructures for mechanical efficiency. *Proc. R. Soc. A* **450**, 141–162 (1995).
35. Deshpande, V. S., Ashby, M. F. & Fleck, N. A. Foam topology: bending versus stretching dominated architectures. *Acta Mater.* **49**, 1035–1040 (2001).
36. Deshpande, V. S., Fleck, N. A. & Ashby, M. F. Effective properties of the octet-truss lattice material. *J. Mech. Phys. Solids* **49**, 1747–1769 (2001).
37. Huber, J. E., Fleck, N. A. & Ashby, M. F. The selection of mechanical actuators based on performance indices. *Proc. R. Soc. A* **453**, 2185–2205 (1997).
38. Ashby, M. Designing architectured materials. *Scr. Mater.* **68**, 4–7 (2013).
39. Sigmund, O. Topology optimization: a tool for the tailoring of structures and materials. *Philos. Trans. R. Soc. A* **358**, 211–227 (2000).
40. Sigmund, O. On the design of compliant mechanisms using topology optimization. *Mech. Struct. Mach.* **25**, 493–524 (1997).
41. Zhao, Z., Kundu, R. D., Sigmund, O. & Zhang, X. S. Extreme nonlinearity by layered materials through inverse design. *Sci. Adv.* **11**, eadr6925 (2025).
42. Pastor-Satorras, R. & Vespignani, A. Epidemic spreading in scale-free networks. *Phys. Rev. Lett.* **86**, 3200–3203 (2001).
43. Pecora, L. M. & Carroll, T. L. Master stability functions for synchronized coupled systems. *Phys. Rev. Lett.* **80**, 2109–2112 (1998).
44. Feld, S. L. Why your friends have more friends than you do. *Am. J. Sociol.* **96**, 1464–1477 (1991).
45. Li, Z. et al. Hardness variation in nanocrystalline SiC irradiated with heavy ions. *Ceram. Int.* **48**, 17846–17851 (2022).
46. Laniel, D. et al. Synthesis of ultra-incompressible and recoverable carbon nitrides featuring CN4 tetrahedra. *Adv. Mater.* **36**, 2308030 (2024).
47. Sigmund, O. Tailoring materials with prescribed elastic properties. *Mech. Mater.* **20**, 351–368 (1995).
This foundational work introduces the method of topology optimization, which remains widely used for metamaterial design.
48. Osanov, M. & Guest, J. K. Topology optimization for architected materials design. *Annu. Rev. Mater. Res.* **46**, 211–233 (2016).
49. Bendsoe, M. P. & Kikuchi, N. Generating optimal topologies in structural design using a homogenization method. *Comput. Methods Appl. Mech. Eng.* **71**, 197–224 (1988).
50. Sylvestre, J. & Morissette, J.-F. Neuromorphic metamaterial structures. *Mater. Des.* **210**, 110078 (2021).
51. Zaiser, M. & Zapperi, S. Disordered mechanical metamaterials. *Nat. Rev. Phys.* **5**, 679–688 (2023).
This perspective describes non-network-based approaches for describing and designing disordered metamaterials.
52. Picu, C. R. *Network Materials: Structure and Properties* (Cambridge Univ. Press, 2022).
This book uses networks to describe fibrous materials, as they naturally capture the free volume typical of biological structures.
53. Hsieh, M.-T., Endo, B., Zhang, Y., Bauer, J. & Valdevit, L. The mechanical response of cellular materials with spinodal topologies. *J. Mech. Phys. Solids* **125**, 401–419 (2019).
54. Ruffini, F. N. & Rimoli, J. J. Asymmetric tension–compression connectivity governs deformation delocalization in truss-based metamaterials. *npj Metamaterials* **2**, 10 (2026).
55. Surjadi, J. U., Aymon, B. F. G., Carton, M. & Portela, C. M. Double-network-inspired mechanical metamaterials. *Nat. Mater.* **24**, 945–954 (2025).
This paper describes the use of interpenetrating networks to design materials with exceptional fracture toughness.
56. Reid, D. R. et al. Auxetic metamaterials from disordered networks. *Proc. Natl Acad. Sci. USA* **115**, E1384–E1390 (2018).
57. Wool, R. P. Rigidity percolation model of polymer fracture. *J. Polym. Sci. B* **43**, 168–183 (2005).
58. Barthélemy, M. Spatial networks. *Phys. Rep.* **499**, 1–101 (2011).
59. Rodgers, N., Tiňo, P. & Johnson, S. Strong connectivity in real directed networks. *Proc. Natl Acad. Sci. USA* **120**, e2215752120 (2023).
60. Fruchart, M., Hanai, R., Littlewood, P. B. & Vitelli, V. Non-reciprocal phase transitions. *Nature* **592**, 363–369 (2021).
61. Watts, D. J. & Strogatz, S. H. Collective dynamics of 'small-world' networks. *Nature* **393**, 440–442 (1998).
62. Barabási, A. L. & Albert, R. Emergence of scaling in random networks. *Science* **286**, 509–512 (1999).
63. Girvan, M. & Newman, M. E. J. Community structure in social and biological networks. *Proc. Natl Acad. Sci. USA* **99**, 7821–7826 (2002).
64. Dorogovtsev, S. N., Goltsev, A. V. & Mendes, J. F. F. Critical phenomena in complex networks. *Rev. Mod. Phys.* **80**, 1275–1335 (2008).
65. Battiston, F. et al. Networks beyond pairwise interactions: structure and dynamics. *Phys. Rep.* **874**, 1–92 (2020).
66. Battiston, F. et al. The physics of higher-order interactions in complex systems. *Nat. Phys.* **17**, 1093–1098 (2021).
67. Bianconi, G. *Multilayer Networks: Structure and Function* (Oxford Univ. Press, 2018).
68. De Domenico, M. et al. Mathematical formulation of multilayer networks. *Phys. Rev. X* **3**, 041022 (2013).
69. Holme, P. & Saramäki, J. Temporal networks. *Phys. Rep.* **519**, 97–125 (2012).
70. Masuda, N. & Lambiotte, R. *A Guide to Temporal Networks*, Vol. 4 (World Scientific, 2016).
71. Eagle, N., Pentland, A. & Lazer, D. Inferring friendship network structure by using mobile phone data. *Proc. Natl Acad. Sci. USA* **106**, 15274–15278 (2009).
72. Barthélemy, M., Boeing, G., Chiaradia, A. & Webster, C. J. Surfacic networks. *PNAS Nexus* **4**, pgae585 (2025).
73. Faloutsos, M., Faloutsos, P. & Faloutsos, C. On power-law relationships of the internet topology. *ACM SIGCOMM Comput. Commun. Rev.* **29**, 251–262 (1999).
74. Weiner, N., Bhosale, Y., Gazzola, M. & King, H. Mechanics of randomly packed filaments—the "bird nest" as meta-material. *J. Appl. Phys.* **127**, 050902 (2020).
75. Hiraoka, Y. et al. Hierarchical structures of amorphous solids characterized by persistent homology. *Proc. Natl Acad. Sci. USA* **113**, 7035–7040 (2016).
76. MacArthur, B. D., Sánchez-García, R. J. & Anderson, J. W. Symmetry in complex networks. *Discrete Appl. Math.* **156**, 3525–3531 (2008).
77. Golubitsky, M. & Stewart, I. Nonlinear dynamics of networks: the groupoid formalism. *Bull. Am. Math. Soc.* **43**, 305–365 (2006).
78. Nicosia, V., Valencia, M., Chavez, M., Díaz-Guilera, A. & Latora, V. Remote synchronization reveals network symmetries and functional modules. *Phys. Rev. Lett.* **110**, 174102 (2013).
79. Nishikawa, T. & Motter, A. E. Symmetric states requiring system asymmetry. *Phys. Rev. Lett.* **117**, 114101 (2016).
80. Krivovichev, S. Structural complexity and configurational entropy of crystals. *Acta Crystallogr. B* **72**, 274–276 (2016).
81. Bianconi, G. Entropy of network ensembles. *Phys. Rev. E* **79**, 036114 (2009).
82. Coolen, A. C. C., Annibale, A. & Roberts, E. S. *Generating Random Networks and Graphs* (Oxford Univ. Press, 2017).
83. Shannon, C. E. A mathematical theory of communication. *Bell Syst. Tech. J.* **27**, 379–423 (1948).
84. Zhang, M., Zhang, B., Ding, J. & Ma, E. Quantifying the local compositional fluctuation and Shannon entropy inherent in multi-principal element alloys. *Scr. Mater.* **259**, 116559 (2025).
85. Torquato, S., Skolnick, M. & Kim, J. Local order metrics for two-phase media across length scales. *J. Phys. A* **55**, 274003 (2022).
86. Maher, C. E. & Newhall, K. A. Characterizing the hyperuniformity of disordered network metamaterials. *Phys. Rev. E* **111**, 65420 (2025).
87. Liu, Y. Z. et al. A generative model of the connectome with dynamic axon growth. *Netw. Neurosci.* **8**, 1192–1211 (2024).
88. Rivera-Alba, M. et al. Wiring economy and volume exclusion determine neuronal placement in the *Drosophila* brain. *Curr. Biol.* **21**, 2000–2005 (2011).
89. Kleinberg, J. M. Navigation in a small world. *Nature* **406**, 845–845 (2000).
90. Amit, G., Ben Porath, D., Buldyrev, S. V. & Bashan, A. Percolation in fractal spatial networks with long-range interactions. *Phys. Rev. Res.* **5**, 023129 (2023).
91. Kosmidis, K., Havlin, S. & Bunde, A. Structural properties of spatially embedded networks. *Europhys. Lett.* **82**, 48005 (2008).
92. Li, D. Q. et al. Percolation of spatially constraint networks. *Europhys. Lett.* **93**, 68004 (2011).
93. Plaszczynski, S., Nakamura, G., Deroulers, C., Grammaticos, B. & Badoual, M. Levy geometric graphs. *Phys. Rev. E* **105**, 054151 (2022).
94. Schmeltzer, C., Soriano, J., Sokolov, I. M. & Rüdiger, S. Percolation of spatially constrained Erdős-Rényi networks with degree correlations. *Phys. Rev. E* **89**, 012116 (2014).
95. Liu, Y., Dehmamy, N. & Barabási, A.-L. Isotopy and energy of physical networks. *Nat. Phys.* **17**, 216–222 (2021).
96. Tubiana, L. et al. Topology in soft and biological matter. *Phys. Rep.* **1075**, 1–137 (2024).
97. Day, T. C. et al. Morphological entanglement in living systems. *Phys. Rev. X* **14**, 011008 (2024).
98. Pete, G., Timár, Á, Stefánsson, S. Ö, Bonamassa, I. & Pósfai, M. Physical networks as network-of-networks. *Nat. Commun.* **15**, 4882 (2024).
99. Meng, X., Piazza, B., Both, C., Barzel, B. & Barabási, A.-L. Surface optimization governs the local design of physical networks. *Nature* **649**, 315–322 (2026).
100. Balister, P., Song, C., Riordan, O., Bollobas, B. & Barabasi, A.-L. Topological phase transitions in spatial networks. Preprint at https://doi.org/10.48550/arXiv.1806.10114 (2018).
101. Emmerich, T., Bunde, A. & Havlin, S. Structural and functional properties of spatially embedded scale-free networks. *Phys. Rev. E* **89**, 062806 (2014).
102. Liu, K., Sun, R. & Daraio, C. Growth rules for irregular architected materials with programmable properties. *Science* **377**, 975–981 (2022).
This work introduces a virtual growth model of metamaterials in which the underlying physical network naturally accommodates tunable disorder and volume exclusion.
103. Heyde, A., Guo, L., Jost, C., Theraulaz, G. & Mahadevan, L. Self-organized biotectonics of termite nests. *Proc. Natl Acad. Sci. USA* **118**, e2006985118 (2021).

104. Frary, M. E. & Schuh, C. A. Correlation-space description of the percolation transition in composite microstructures. *Phys. Rev. E* **76**, 041108 (2007).
This article shows that additive descriptors are insufficient to capture properties associated with the percolation transition, as short-range order alters the percolation threshold.
105. Mecke, K. R. in *Statistical Physics and Spatial Statistics*, Vol. 554 (eds Mecke, K. R. & Stoyan, D.) **554**, 111–184 (Springer, 2000).
106. Nocedal, J. & Wright, S. J. *Numerical Optimization* (Springer, 2006).
107. Berneman, M. & Hexner, D. Designing precise dynamical steady states in disordered networks. *Mach. Learn. Sci. Technol.* **6**, 025073 (2025).
108. Nicolaou, Z. G. & Motter, A. E. Mechanical metamaterials with negative compressibility transitions. *Nat. Mater.* **11**, 608–613 (2012).
109. D'Amico, A., Tu, S. & Singh, A. Topological insights into dense frictional suspension rheology: third-order loops drive discontinuous shear thickening. *J. Chem. Phys.* **162**, 214906 (2025).
110. Aminimajd, A., Maia, J. & Singh, A. Robust prediction of frictional contact network in near-jamming suspensions employing deep graph neural networks. *Phys. Fluids* **37**, 73306 (2025).
111. Colen, J. et al. Machine learning active-nematic hydrodynamics. *Proc. Natl Acad. Sci. USA* **118**, e2016708118 (2021).
112. Schmitt, M. S. et al. Machine learning interpretable models of cell mechanics from protein images. *Cell* **187**, 481–494 (2024).
113. Kipf, T. N. & Welling, M. Semi-supervised classification with graph convolutional networks. Preprint at https://doi.org/10.48550/arXiv.1609.02907 (2017).
114. Reiser, P. et al. Graph neural networks for materials science and chemistry. *Commun. Mater.* **3**, 93 (2022).
115. Batzner, S. et al. E(3)-equivariant graph neural networks for data-efficient and accurate interatomic potentials. *Nat. Commun.* **13**, 2453 (2022).
116. Ha, C. S. et al. Rapid inverse design of metamaterials based on prescribed mechanical behavior through machine learning. *Nat. Commun.* **14**, 5765 (2023).
117. Jin, H. et al. Characterization and inverse design of stochastic mechanical metamaterials using neural operators. *Adv. Mater.* **37**, 2420063 (2025).
118. Kingma, D. P. & Welling, M. Auto-encoding variational Bayes. Preprint at https://doi.org/10.48550/arXiv.1312.6114 (2022).
119. Zheng, L., Karapiperis, K., Kumar, S. & Kochmann, D. M. Unifying the design space and optimizing linear and nonlinear truss metamaterials by generative modeling. *Nat. Commun.* **14**, 7563 (2023).
120. Grover, A., Zweig, A. & Ermon, S. Graphite: iterative generative modeling of graphs. In *Proc. 36th International Conference on Machine Learning* (eds Chaudhuri, K. & Salakhutdinov, R.) 2434–2444 (ML Research Press, 2019).
121. Mandal, R., Casert, C. & Sollich, P. Robust prediction of force chains in jammed solids using graph neural networks. *Nat. Commun.* **13**, 4424 (2022).
122. Bapst, V. et al. Unveiling the predictive power of static structure in glassy systems. *Nat. Phys.* **16**, 448–454 (2020).
123. Meyer, P. P., Bonatti, C., Tancogne-Dejean, T. & Mohr, D. Graph-based metamaterials: deep learning of structure-property relations. *Mater. Des.* **223**, 111175 (2022).
This article provides a scheme for expressing shell metamaterials in terms of networks.
124. Bastek, J.-H., Kumar, S., Telgen, B., Glaesener, R. N. & Kochmann, D. M. Inverting the structure–property map of truss metamaterials by deep learning. *Proc. Natl Acad. Sci. USA* **119**, e2111505119 (2022).
125. Bonfanti, S. et al. Computational design of mechanical metamaterials. *Nat. Comput. Sci.* **4**, 574–583 (2024).
This perspective outlines both the computational and fabrication challenges associated with realizing metamaterial designs.
126. Woldseth, R. V., Aage, N., Bærentzen, J. A. & Sigmund, O. On the use of artificial neural networks in topology optimisation. *Struct. Multidiscip. Optim.* **65**, 1–36 (2022).
127. Both, C., Dehmamy, N., Yu, R. & Barabási, A.-L. Accelerating network layouts using graph neural networks. *Nat. Commun.* **14**, 1560 (2023).
128. Boguñá, M. et al. Network geometry. *Nat. Rev. Phys.* **3**, 114–135 (2021).
129. van Saarloos, W., Vitelli, V. & Zeravcic, Z. *Soft Matter: Concepts, Phenomena, and Applications* 433–440 (Princeton Univ. Press, 2024).
130. Jaeger, H. M., Murugan, A. & Nagel, S. R. Training physical matter to matter. *Soft Matter* **20**, 6695–6701 (2024).
131. Stern, M. & Murugan, A. Learning without neurons in physical systems. *Annu. Rev. Condens. Matter Phys.* **14**, 417–441 (2023).
132. Stern, M., Hexner, D., Rocks, J. W. & Liu, A. J. Supervised learning in physical networks: from machine learning to learning machines. *Phys. Rev. X* **11**, 021045 (2021).
133. Liu, W., Sigalov, T. A., Coulais, C. & Shokef, Y. Combinatorial design of floppy modes and frustrated loops in metamaterials. *Phys. Rev. Lett.* **136**, 038202 (2026).
134. Mandal, R. et al. Learning dynamical behaviors in physical systems. Preprint at https://doi.org/10.48550/arXiv.2406.07856 (2024).
135. Wright, L. G. et al. Deep physical neural networks trained with backpropagation. *Nature* **601**, 549–555 (2022).
This article recognizes that physical responses can be leveraged to perform backpropagation computations that optimize material properties.
136. Momeni, A. et al. Training of physical neural networks. *Nature* **645**, 53–61 (2025).
137. Gibson, I. et al. *Additive Manufacturing Technologies*, Vol. 17 (Springer, 2021).
138. Zhou, W. J. et al. 3D polycatenated architected materials. *Science* **387**, 269–277 (2025).
139. Guo, Y. et al. Minimal surface-based materials for topological elastic wave guiding. *Adv. Funct. Mater.* **32**, 2204122 (2022).
140. Zhu, C. et al. Highly compressible 3D periodic graphene aerogel microlattices. *Nat. Commun.* **6**, 6962 (2015).
141. Pürstl, J. T. et al. Geometry-assisted phase selection: interplay of phase heterogeneity and geometry in gyroid shell metamaterials printed with 17-4 PH stainless steel. *Adv. Eng. Mater.* **27**, 2402309 (2025).
142. Cheben, P., Halir, R., Schmid, J. H., Atwater, H. A. & Smith, D. R. Subwavelength integrated photonics. *Nature* **560**, 565–572 (2018).
143. Guell Izard, A., Bauer, J., Crook, C., Turlo, V. & Valdevit, L. Ultrahigh energy absorption multifunctional spinodal nanoarchitectures. *Small* **15**, 1903834 (2019).
144. Baldacchini, T. *Three-Dimensional Microfabrication Using Two-Photon Polymerization: Fundamentals, Technology, and Applications* (William Andrew, 2015).
145. Vyatskikh, A. et al. Additive manufacturing of 3D nano-architected metals. *Nat. Commun.* **9**, 593 (2018).
146. Bauer, J., Sala-Casanovas, M., Amiri, M. & Valdevit, L. Nanoarchitected metal/ceramic interpenetrating phase composites. *Sci. Adv.* **8**, eabo3080 (2022).
147. Bauer, J., Crook, C. & Baldacchini, T. A sinterless, low-temperature route to 3D print nanoscale optical-grade glass. *Science* **380**, 960–966 (2023).
148. Shaikeea, A. J. D., Cui, H., O'Masta, M., Zheng, X. R. & Deshpande, V. S. The toughness of mechanical metamaterials. *Nat. Mater.* **21**, 297–304 (2022).
149. Garcia, A. E. et al. Scalable synthesis of gyroid-inspired freestanding three-dimensional graphene architectures. *Nanoscale Adv.* **1**, 3870–3882 (2019).
150. Zhang, Y., Hsieh, M.-T. & Valdevit, L. Mechanical performance of 3D printed interpenetrating phase composites with spinodal topologies. *Compos. Struct.* **263**, 113693 (2021).
151. Shen, M. et al. An autonomous design algorithm to experimentally realize three-dimensionally isotropic auxetic network structures without compromising density. *npj Comput. Mater.* **10**, 113 (2024).
152. Milkus, R. & Zaccone, A. Local inversion-symmetry breaking controls the boson peak in glasses and crystals. *Phys. Rev. B* **93**, 094204 (2016).
153. Hain, T., Santangelo, C. & Manning, M. L. Optimizing properties on the critical rigidity manifold of underconstrained central-force networks. *Phys. Rev. E* **111**, 015418 (2025).
154. Nguyen, C., Peetz, D., Elbanna, A. E. & Carlson, J. M. Characterization of fracture in topology-optimized bioinspired networks. *Phys. Rev. E* **100**, 042402 (2019).
155. Berthier, E., Porter, M. A. & Daniels, K. E. Forecasting failure locations in 2-dimensional disordered lattices. *Proc. Natl Acad. Sci. USA* **116**, 16742–16749 (2019).
156. Wang, R.-S., Saadatpour, A. & Albert, R. Boolean modeling in systems biology: an overview of methodology and applications. *Phys. Biol.* **9**, 055001 (2012).
157. Barrat, A., Barthélemy, M. & Vespignani, A. *Dynamical Processes on Complex Networks* (Cambridge Univ. Press, 2008).
158. Boattini, E., Smallenburg, F. & Filion, L. Averaging local structure to predict the dynamic propensity in supercooled liquids. *Phys. Rev. Lett.* **127**, 088007 (2021).
159. Jung, G., Biroli, G. & Berthier, L. Predicting dynamic heterogeneity in glass-forming liquids by physics-inspired machine learning. *Phys. Rev. Lett.* **130**, 238202 (2023).
160. Florijn, B., Coulais, C. & van Hecke, M. Programmable mechanical metamaterials. *Phys. Rev. Lett.* **113**, 175503 (2014).
161. Chen, T., Pauly, M. & Reis, P. M. A reprogrammable mechanical metamaterial with stable memory. *Nature* **589**, 386–390 (2021).
162. Fulco, S., Budzik, M. K., Xiao, H., Durian, D. J. & Turner, K. T. Disorder enhances the fracture toughness of 2D mechanical metamaterials. *PNAS Nexus* **4**, pgaf023 (2025).
163. Artime, O. et al. Robustness and resilience of complex networks. *Nat. Rev. Phys.* **6**, 114–131 (2024).
164. Luan, S., Chen, E., John, J. & Gaitanaros, S. A data-driven framework for structure-property correlation in ordered and disordered cellular metamaterials. *Sci. Adv.* **9**, eadi1453 (2023).
165. Blagojević, L. & Pósfai, M. Three-dimensional shape and connectivity of physical networks. *Sci. Rep.* **14**, 16874 (2024).
166. Papadopoulos, L., Porter, M. A., Daniels, K. E. & Bassett, D. S. Network analysis of particles and grains. *J. Complex Netw.* **6**, 485–565 (2018).
167. Xia, X., Spadaccini, C. M. & Greer, J. R. Responsive materials architected in space and time. *Nat. Rev. Mater.* **7**, 683–701 (2022).
168. Pang, J. C. et al. Geometric constraints on human brain function. *Nature* **618**, 566–574 (2023).
169. Ercsey-Ravasz, M. et al. A predictive network model of cerebral cortical connectivity based on a distance rule. *Neuron* **80**, 184–197 (2013).
170. Wang, X., Li, X., Li, Z., Wang, Z. & Zhai, W. Superior strength, toughness, and damage-tolerance observed in microlattices of aperiodic unit cells. *Small* **20**, e2307369 (2024).
171. Wang, G., Jiao, P., Bai, J. & Chen, Z. Quasi-isotropy in non-periodic metastructures and topological solution for directional freedom. *Thin-Walled Struct.* **214**, 113396 (2025).
172. Siedentop, L. et al. Stealthy and hyperuniform isotropic photonic band gap structure in 3D. *PNAS Nexus* **3**, pgae383 (2024).
This work leverages hyperuniformity to design 3D metamaterial structures with isotropic photonic bandgaps.
173. Arns, C. H., Knackstedt, M. A., Pinczewski, W. V. & Mecke, K. R. Euler-Poincaré characteristics of classes of disordered media. *Phys. Rev. E* **63**, 031112 (2001).
This article is an early example of unifying the description of a broad class of material systems under a common set of descriptors, namely, Minkowski functionals.

174. Surjadi, J. U. et al. Exploiting multiscale dynamic toughening in multicomponent alloy metamaterials for extreme impact mitigation. *Sci. Adv.* **11**, eadt0589 (2025).
175. Cormier, Y., Dupuis, P., Farjam, A., Corbeil, A. & Jodoin, B. Additive manufacturing of pyramidal pin fins: height and fin density effects under forced convection. *Int. J. Heat Mass Transf.* **75**, 235–244 (2014).
176. Laghi, V., Palermo, M., Gasparini, G. & Trombetti, T. Computational design and manufacturing of a half-scaled 3D-printed stainless steel diagrid column. *Addit. Manuf.* **36**, 101505 (2020).
177. Saccone, M. A., Gallivan, R. A., Narita, K., Yee, D. W. & Greer, J. R. Additive manufacturing of micro-architected metals via hydrogel infusion. *Nature* **612**, 685–690 (2022).
178. Zheng, X. et al. Multiscale metallic metamaterials. *Nat. Mater.* **15**, 1100–1106 (2016).
179. Shi, S., Li, Y., Ngo-Dinh, B.-N., Markmann, J. & Weissmüller, J. Scaling behavior of stiffness and strength of hierarchical network nanomaterials. *Science* **371**, 1026–1033 (2021).
180. Hatton, B., Mishchenko, L., Davis, S., Sandhage, K. H. & Aizenberg, J. Assembly of large-area, highly ordered, crack-free inverse opal films. *Proc. Natl Acad. Sci. USA* **107**, 10354–10359 (2010).
181. Neophytou, A., Chakrabarti, D. & Sciortino, F. Topological nature of the liquid–liquid phase transition in tetrahedral liquids. *Nat. Phys.* **18**, 1248–1253 (2022).
182. Neophytou, A., Starr, F. W., Chakrabarti, D. & Sciortino, F. Hierarchy of topological transitions in a network liquid. *Proc. Natl Acad. Sci. USA* **121**, e2406890121 (2024).
183. Gutiérrez Fosado, Y. A., Michieletto, D. & Martelli, F. Link to densify: topological transitions and origin of hysteresis during the compression and decompression of amorphous ices. *Phys. Rev. Lett.* **133**, 266102 (2024).
184. Palombo, G., Weir, S., Michieletto, D. & Gutiérrez Fosado, Y. A. Topological linking determines elasticity in limited valence networks. *Nat. Mater.* **24**, 454–461 (2025).
185. Bonamassa, I. et al. Logarithmic kinetics and bundling in random packings of elongated 3D physical links. *Proc. Natl Acad. Sci. USA* **122**, e2427145122 (2025).
186. Glover, C. & Barabási, A. L. Measuring entanglement in physical networks. *Phys. Rev. Lett.* **133**, 077401 (2024).
187. Chen, Y., Fleury, R., Seppecher, P., Hu, G. & Wegener, M. Nonlocal metamaterials and metasurfaces. *Nat. Rev. Phys.* **7**, 299–312 (2025).
188. Kim, J. Z., Lu, Z., Blevins, A. S. & Bassett, D. S. Nonlinear dynamics and chaos in conformational changes of mechanical metamaterials. *Phys. Rev. X* **12**, 011042 (2022).
189. Krizhevsky, A., Sutskever, I. & Hinton, G. E. ImageNet classification with deep convolutional neural networks. *Commun. ACM* **60**, 84–90 (2017).
190. Hinton, G. et al. Deep neural networks for acoustic modeling in speech recognition: the shared views of four research groups. *IEEE Signal Process. Mag.* **29**, 82–97 (2012).
This article offers a perspective on how CNNs achieve record-breaking accuracy in speech processing tasks.
191. Scarselli, F., Gori, M., Tsoi, A. C., Hagenbuchner, M. & Monfardini, G. The graph neural network model. *IEEE Trans. Neural Netw.* **20**, 61–80 (2009).
This paper is among the first to propose GNNs, relate them to other architectures and describe how they can be trained.
192. Bronstein, M. M., Bruna, J., Cohen, T. & Veličković, P. Geometric deep learning: grids, groups, graphs, geodesics, and gauges. Preprint at https://doi.org/10.48550/arXiv.2104.13478 (2021).

Acknowledgements
The authors thank C. Fox for providing images of metamaterial samples and E. Gokmen, K.M. Ainger, E. Stanifer and Y. Zhao for insightful discussions.

Author contributions
All authors contributed substantially to the discussion of the content. T.P.W. and A.E.M. led the writing of the article. All authors reviewed and/or edited the manuscript before submission.

Funding
This work was supported by MURI ARO grant no. W911NF-22-20109.

Competing interests
The authors declare no competing interests.

Additional information
Supplementary information The online version contains supplementary material available at https://doi.org/10.1038/s41578-026-00936-0.

Peer review information *Nature Reviews Materials* thanks the anonymous reviewers for their contribution to the peer review of this work.

Publisher's note Springer Nature remains neutral with regard to jurisdictional claims in published maps and institutional affiliations.